Mitigating Short-Term Variations of Photovoltaic Generation Using Energy Storage with VOLTTRON

Kevin Morrissey

A thesis

submitted in partial fulfillment of the

requirements for the degree of

Master of Science in Electrical Engineering

University of Washington

2017

Reading Committee:

Miguel A. Ortega-Vazquez, Chair

Daniel S. Kirschen

Program Authorized to Offer Degree:

Electrical Engineering

Abstract

Mitigating Short-Term Variations of Photovoltaic Generation Using Energy Storage with VOLTTRON

Kevin Morrissey

University of Washington

Chair of the Supervisory Committee:

Assistant Professor Miguel A. Ortega-Vazquez

Electrical Engineering Department

A smart-building communications system performs smoothing on photovoltaic (PV) power generation using a battery energy storage system (BESS). The system runs using VOLTTRON™, a multi-agent python-based software platform dedicated to power systems. The VOLTTRON™ system designed for this project runs synergistically with the larger University of Washington VOLTTRON™ environment, which is designed to operate UW device communications and databases as well as to perform real-time operations for research. One such research algorithm that operates simultaneously with this PV Smoothing System is an energy cost optimization system which optimizes net demand and associated cost throughout a day using the BESS. The PV Smoothing System features an active low-pass filter with an adaptable time constant, as well as adjustable limitations on the output power and accumulated battery energy of the BESS contribution.

The system was analyzed using 26 days of PV generation at 1-second resolution. PV smoothing was studied with unconstrained BESS contribution as well as under a broad range of BESS constraints analogous to variable-sized storage. It was determined that a large inverter output power was more important for PV smoothing than a large battery energy capacity. Two methods of selecting the time constant in real time, static and adaptive, are studied for their impact on system performance. It was found that both systems provide a high level of PV smoothing performance, within 8% of the ideal case where the best time constant is known ahead of time. The system was run in real time using VOLTTRON™ with BESS limitations of 5 kW/6.5 kWh and an adaptive update period of 7 days. The system behaved as expected given the BESS parameters and time constant selection methods, providing smoothing on the PV generation and updating the time constant periodically using the adaptive time constant selection method.

Table of Contents

List of Figures

List of Tables

Acknowledgments

I Introduction

Growth of renewable energy generation is forecasted to continue to increase in the coming years due its improving economic viability, coupled with concern over the polluting nature of burning fossil fuels. Many U.S. states have set goals for the portion of generation attributed to clean, renewable sources and have enacted plans to grow the base of renewable generation [1]. This has spurred the construction of many new renewable plants and an increase in distributed rooftop solar installments, and renewable generation capacity has grown rapidly both in the U.S. and at a global scale [2]. However, increased generation base is only part of the solution - with higher penetration of renewable sources, there also comes increased uncertainty and variation in the power system. High penetrations of stochastic wind and solar generation require more considerations in terms of grid flexibility and storage, as is discussed in [3].

Renewable sources bring with them inherent uncertainty as they are reliant on natural forces and weather patterns. There is uncertainty on the scale of hours and days, where forecasts may be inaccurate and generation may not match what was predicted. Wind generation is not as variable as solar because it relies on a spinning rotor which has inertia, and the turbines generally feature pitch control which keeps a constant power within a range of wind speeds. With solar generation, there is also uncertainty on the scale of seconds, where sunlight is subject to small stochastic noise-like variations throughout the day. Take, for example, a cloud of varying density passing in front of the sun – a solar farm may see a decrease in generation from the cloud cover on an otherwise blue sky, and then experience vast fluctuations based on the density of the cloud as it passes. This short-term variability requires increased flexibility and reserve on power system in order to balance the load and generation, and often involves a high-cost peaking gas turbine to quickly resolve mismatches in generation and load [4].

Many proposed solutions to the broad issue of renewable generation uncertainty and variation include the installation of grid-level storage [5]. One of the applications of such storage is performing smoothing on solar generation to decrease variations occurring on the order of seconds. This involves absorbing the fluctuations using a filtering mechanism so that generated power ramps up and down more slowly. Output is still governed by stochastic and uncertain phenomena, but a more stable and slow-changing characteristic greatly improves the ability of the grid to accommodate solar generation.

PV smoothing does not always directly benefit the owner of the panels. While making the PV output of a distributed installation more stable may slightly improve the voltage and power quality on the distribution branch, the largest benefits are seen by the utility, balancing authority, and the generating units. Short-term power imbalances must be compensated by adjusting output on other generators in the system, which, and the units capable of fast adjustment are often some of the more expensive units. Because of this,

monetization of PV smoothing depends heavily on the system in which the PV array is installed, and will differ depending on the flexibility and quantity of the units available. PV smoothing would likely be installed for a distributed PV array with incentive given by the regional utility benefitting from the smoothing functions.

Larger systems fare better in terms of flexibility, as the aggregation of loads and generation from a large region are better able to accommodate variations from a solar plant. In addition, some degree of smoothing occurs naturally among PV plants spread out across geographic locations [6]. Regionally aggregated natural PV smoothing is not considered for this project.

Presented is a filtering system designed to smooth variations in solar generation on the second scale. The solar generation is a 35-kW array located on the roof of a building at the University of Washington (UW). The system makes use of a 100 kW/325 kWh battery energy storage system (BESS) located in the basement of another campus building. The system makes use of the VOLTTRON™ building platform: an open-sourced, python-based communications system developed at Pacific Northwest National Laboratory (PNNL) for the control and monitoring of building energy systems. VOLTTRON™ presents an opportunity to create uniquely customizable controls for building and campus energy management networks. The VOLTTRON™ solution includes central control and filtering functions as well as driver interfaces with the hardware elements. The smoothing system operates synchronously and simultaneously with the larger UW VOLTTRON™ environment, which is designed to operate UW device communications and databases as well as to perform research algorithms. One such research algorithm that operates simultaneously with this PV Smoothing System is an energy cost optimization system which optimizes net demand and associated cost throughout a day using the BESS. This requires real-time coordination to jointly operate the BESS between the two research systems.

This project investigates an active low-pass filter approach to smoothing the PV generation. Various filters time constants, which correspond to different levels of smoothing, are analyzed. Additionally, an adaptive approach where historical data is used to adapt the filter time constant in real time is investigated. The contribution of the BESS in terms of inverter power and battery energy is varied to determine the parameters of storage necessary to perform smoothing. A 26-day period of PV measurement data at 1-second resolution is analyzed among various time constants and BESS parameters, and two methods of time constant selection are analyzed and compared. Finally, the system is implemented in real time in the VOLTTRON™ environment to demonstrate feasibility.

II VOLTTRON™ Platform

VOLTTRON™ is an open-sourced python-based platform for enabling inter- and intra-building communication. Developed by PNNL, its applications span a wide array of building device monitoring, control, and communication. The platform enables functions such as load peak shaving, temperature setpoint modification, optimization of energy resource allocation, transactive control and data management, and operation of building devices. VOLTTRON™ is being used widely in both academic and industrial purposes as a building energy management and control system, and is as flexible and scalable as the implementation requires [7].

VOLTTRON™ operates on the use of agents, each of which is a python class performing a task. In this way, many operations can run simultaneously, managing several parts of a larger system at once. This allows VOLTTRON™ to be used in real time building operation functions.

2.1 Photovoltaic Smoothing System Architecture in VOLTTRON™

The VOLTTRON™ implementation for this project is shown in Figure 1.
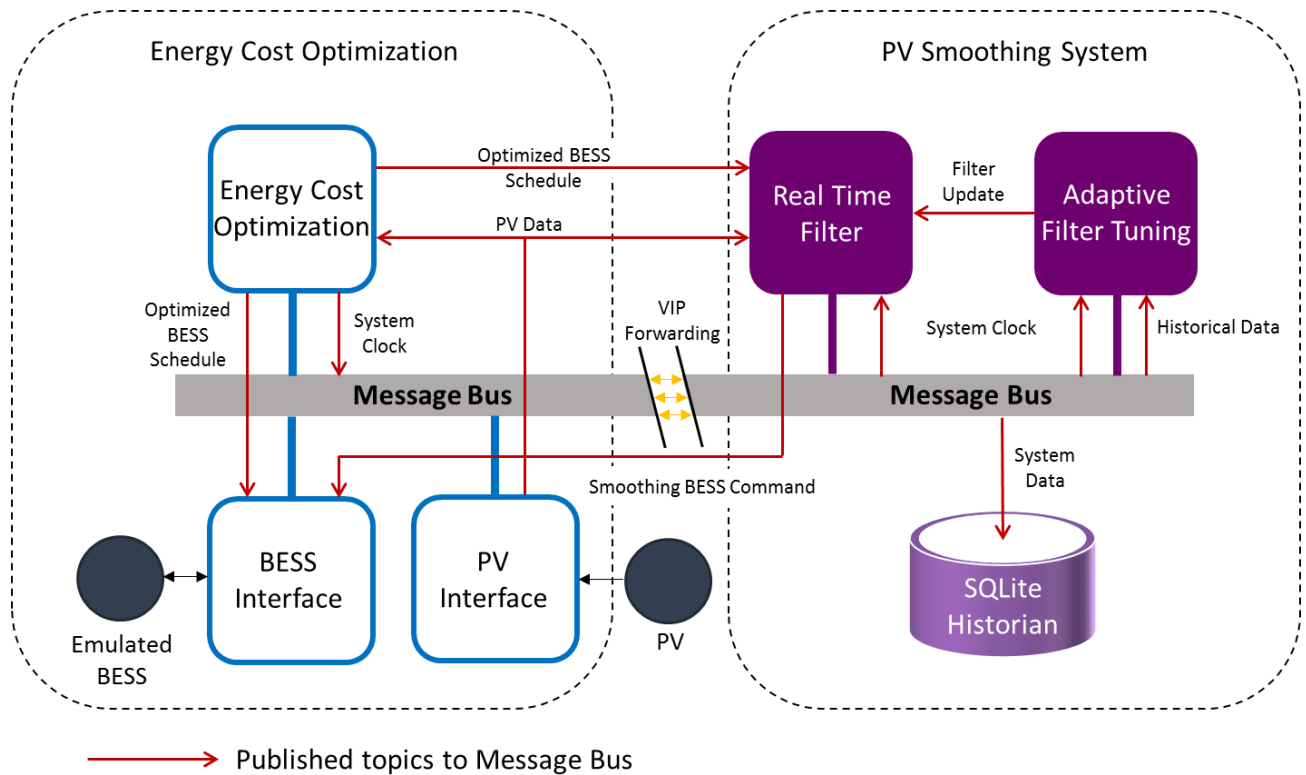
Figure 1: VOLTTRON™ Agent Architecture

The VOLTTRON™ system is divided between two VOLTTRON™ platforms: the Energy Cost Optimization System and the PV Smoothing System. The Energy Cost Optimization System is located on a central workstation, while the PV Smoothing System is located on a peripheral computer. In this configuration, the two separate VOLTTRON™ platforms have their own message bus for agent communication, while they are able to share important cross-platform messages as well.

The two systems communicate using the VOLTTRON™ Interconnect Protocol (VIP). Each platform features a forwarding agent that contains the network address and security credentials of the other platform, enabling them to exchanged published topics containing operations information at each time step.

The Energy Cost Optimization System and PV Smoothing System both exist within the greater UW VOLTTRON™ environment, which manages distributed energy resources and ongoing research functions. At the time of this project, these functions include:

- PV data acquisition using the "Master Driver" agent from 4 PV arrays (140 kW total) on campus.
- Communication and data sharing between VOLTTRON™ instances among partner testbeds.
- MySQL database management using a custom "Selective Historian" agent – which sorts device readings into respective MySQL databases depending on their use.
- Weather data aggregation from Weather Underground using their application program interface (API).
- Energy cost optimization: a research project using building net demand and modeled electricity price forecasts to optimize BESS dispatch at a 5-minute resolution.

In Figure 1, the Energy Cost Optimization System is simplified to show the agents and messages that are important for the PV Smoothing System. This includes the PV data acquisition from the 35 kW array, the BESS interface, and an agent representing the rest of the interconnecting UW environment.

The PV Smoothing System platform comprises the algorithms hereafter described. The system receives the system clock from the central Energy Cost Optimization System, as well as PV power measurement data published every second. The Real Time Filtering Agent accumulates PV measurements and the optimized BESS schedule from the Energy Cost Optimization System and determines an appropriate BESS adjustment for perform smoothing on the generated power. At a specified interval, the Filter Tuning Agent determines a new filter and sends an update to the Real Time Filtering Agent. Data is stored in real time by a SQLite Historian.

III   Literature Review

A large body of work exists on the subject of variability of renewable energy and smoothing solutions to this problem. While VOLTTRON™ is a relatively new platform, introduced as a prototype in 2012, there are some publications out regarding demonstrations and implementations of the smart-building software environment.

3.1   Uncertainty and Variability of Solar Generation

There are numerous papers published on the subject of characterizing and predicting the variations exhibited by renewable energy resources, especially PV and wind generation. [6] is a detailed study on the variability of PV plant output due to cloud cover, discussing the effects of PV plant size and geographic diversity on variability. The authors found that aggregating PV generation over a wide area produces a smoothing effect, as some variations are averaged out of the net generation. In addition, larger installations and indeed larger power systems are more resilient to these variations.

Other papers, such as [3] and [4], discuss the integration costs associated with bringing PV plants online, as well as the factors involved with improving the flexibility and transmission capacity of the grid in response to introduction of highly variable PV power.

[8] discusses PV generation forecasting using a neural network with historical data. The model uses predicted cloud cover to estimate the solar irradiance, temperature, and power output of the PV modules. It goes on to incorporate these predictions into a building load scheme such that the power taken from the grid for temperature regulation can be predicted and optimized.

[9] discusses the power spectral density of wind generation and locating frequency patterns where they exist. This can be applied to PV generation as well.

3.2   Photovoltaic Smoothing

In [10], a 53-kW concentrating PV array is smoothed using a simulated BESS. The filtering mechanism is done using a moving average algorithm. The paper performs smoothing on 1 day of data at a 1-minute resolution, and compares these results with a shorter 20-minute dataset sampled at 1 second. The authors concluded that installing the BESS reduced the maximum ramp rate of the plant, and that a 1-minute resolution does not consider shorter timeframe variations that were captured by the 1-second resolution.

[11] also considers a moving average, though this paper uses a double moving average to perform smoothing on measured data. Not only is the purpose of this paper to reduce fluctuations of PV generation

for grid integration, but also to maximize maximum power point tracking algorithms in the inverter which may not handle fast variations very well.

[12] considers a much larger system, with 1.26 MW of PV installation alongside a 3 MW wind turbine and a 1 MW/MWh BESS. It discusses the trade-off between battery effort and degree of smoothness, a concept that is also explored in this project. It simulates operations of two methods of smoothing the net system power over 50 minutes: one using a dynamic low-pass filtering approach, and one featuring a power fluctuation direct rate limiting approach. In both cases, the objective was to limit the power fluctuations from increasing beyond a specified target. Additional investigations in this study included methods of keeping the BESS in the linear region of its state of charge (SOC), and analyzing a large 40 MW PV system over the course of an entire day.

[13] considers the optimal sizing of BESS, solar, and wind resources, including performing smoothing on the net generation using a second order low pass filter approach. The paper optimizes the system over four different objectives, including cost of operating the system and generation revenues. It features a case study of a system located in China and simulation results, enforcing a maximum ramp rate for the net generation.

In [14], the authors look at generation shifting and ramp rate limiting of an existing wind installation using control of an installed sodium sulfur battery. The smoothing is performed using a low-pass filter approach at 1-minute resolution over the course of a day. The paper goes on to analyze the minute to minute ramp rates, evaluating the smoothness of the result with a histogram showing frequency of different ramp levels. The authors also make the assertion that using the low-pass filter, the ramp rate of the total system is limited to twice the maximum generator output divided by the filter time constant.

[15] considers the use of lead acid battery cells for smoothing, demonstrating system feasibility. The paper studies the effect on battery lifetime of the smoothing function over the course of 30 days.

[16] is a study on several ways a BESS can improve and enable the integration of distributed PV generation. The authors analyze PV smoothing using a BESS unit as part of an installed testbed, enforcing a maximum ramp rate on the system. In addition, the authors consider auxiliary services that may be provided by a BESS, such as frequency droop response and reactive power support.

[17] discusses the scenario where wind power variability is compensated both by a BESS as well as co-located natural gas generation. The objective of the research is to minimize the BESS requirements while providing the lowest cost energy within smoothness constraints.

3.3 VOLTTRON™ Implementations

Several VOLTTRON™ implementations and examples have been published. PNNL introduces VOLTTRON™ in 2012 in [18], outlining various aspects of its functionality and numerous example applications. In 2013, the same team demonstrated a simple implementation of a smart grid demand response application, described in [19].

[20] describes an implementation aimed at optimizing building loads for temperature control using the real time platform. Demonstration of the VOLTTRON™ system for a research application was an important aspect of that publication.

[21] provides instructional discussion on installing and running VOLTTRON™ on small BeagleBone devices for the purposes of testing and benchmarking the system's device scraping capabilities.

[22] discusses managing distributed energy resources in a broad multi-campus testbed environment for the CETC project, including transactive control communications.

More VOLTTRON™ use cases can be found at DOE's VOLTTRON™ website [7].

IV   System Description

Study of the existing work is an important step in the formulation of a PV smoothing project such as this. There exist several strategies for smoothing PV generation, though the algorithms can be grouped into two families: low-pass filter approaches [10][12][13][14] and ramp rate constraint approaches [12][16][17]. While low-pass filter approaches focus on using past measurements to generate a smooth net output value for the next time step, ramp rate constraint approaches place a strict limit on the amount the output can change in a given time-step and bring the BESS to contribute when this constraint is violated.

Selection of one approach or the other depends on the objective of the smoothing, as well as the available BESS resources. The ramp rate constraint approach is useful as net generation ramping policies can be written into contracts with PV installments, enforcing boundaries on the output of the plant. However, enforcing a strict constraint involves installing a BESS capable of ramping nearly the entire capacity of the installment under worst-case conditions. For the purposes of analyzing the effect of BESS parameters on the overall smoothness of the output, the low-pass filter approach is more suitable as the BESS can be sized smaller than the PV plant capacity and the results will be continuous.

These two approaches can be combined. While this study implements a low-pass filter approach, a strict constraint is programmed into the VOLTTRON™ system in the case this becomes necessary for implementation and study. The block diagram for the filter algorithm is shown in Figure 2.
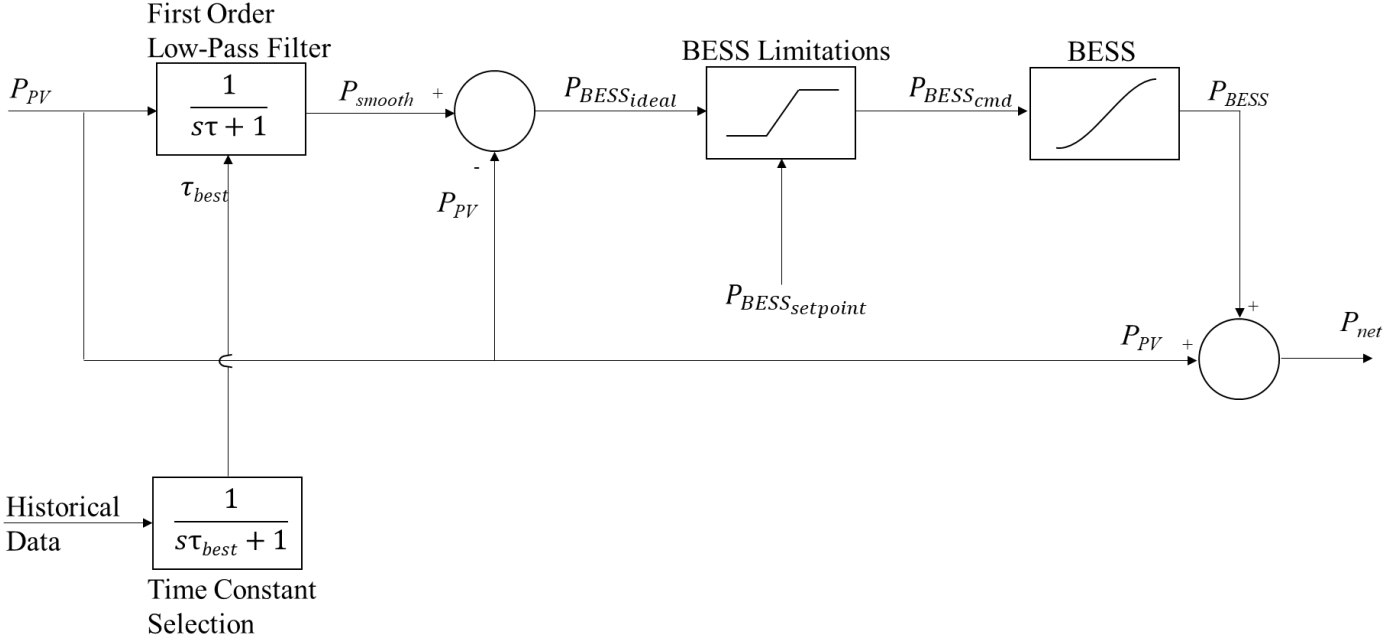
Figure 2: Filter Block Diagram

P_{PV} – measured PV generation

P_{smooth} – Ideal filtered PV generation

$P_{BESS_{ideal}}$ – Ideal BESS contribution to attain the signal P_{smooth}

$P_{BESS_{setpoint}}$ – The current setpoint of the BESS inverter output

$P_{BESS_{cmd}}$ – Command sent to BESS to initiate PV smoothing output

P_{BESS} – Output power of BESS

P_{net} – Net generation of PV Smoothing System

τ – Filter time constant

τ_{best} – Best filter time constant based on historical data

This project uses a time scale of 1 second in order to capture the fast-moving fluctuations in PV generation, as [10] recommends in its study.

The system is described by the following equations:

1st Order Low-Pass Filter:

$$P_{smooth} = P_{PV} * \delta(t) \qquad\qquad\qquad\qquad\qquad \mathbf{1}$$

$\delta()$ – Impulse response of filter transfer function

$$P_{BESS_{ideal}} = P_{smooth} - P_{PV} \qquad\qquad 2$$

BESS Limitations:

$$P_{BESS_{max}} = \min(P_{BESS_{+capacity}}, P_{BESS_{setpoint}} + P_{window}) \qquad\qquad 3$$

$$P_{BESS_{min}} = \max(P_{BESS_{-capacity}}, P_{BESS_{setpoint}} - P_{window}) \qquad\qquad 4$$

i. If $P_{BESS_{ideal}} \geq P_{BESS_{max}}$ $\qquad\qquad$ **5**

$$P_{BESS_{lim}} = P_{BESS_{max}}$$

ii. Else If $P_{BESS_{ideal}} \leq P_{BESS_{min}}$ $\qquad\qquad$ **6**

$$P_{BESS_{lim}} = P_{BESS_{min}}$$

iii. Else $\qquad\qquad$ **7**

$$P_{BESS_{lim}} = P_{BESS_{ideal}}$$

$$E_{max} = \min(E_{capacity}, SOC \times E_{capacity} + E_{window}/2) \qquad\qquad 8$$

$$E_{min} = \max(0, SOC \times E_{capacity} - E_{window}/2) \qquad\qquad 9$$

i. If $E_{BESS} + P_{BESS_{lim}} \times t > E_{max}$ $\qquad\qquad$ **10**

$$P_{BESS_{cmd}} = \frac{E_{max} - E_{BESS}}{t}$$

ii. Else If $E_{BESS} + P_{BESS_{lim}} \times t < E_{min}$ $\qquad\qquad$ **11**

$$P_{BESS_{cmd}} = \frac{E_{min} - E_{BESS}}{t}$$

iii. Else $\qquad\qquad$ **12**

$$P_{BESS_{cmd}} = P_{BESS_{lim}}$$

$P_{BESS_{setpoint}}$ *– Preferred BESS operating point, imported from Energy Cost Optimization System*

$P_{capacity}$ *– Installed inverter capacity*

P_{window} *– Allowable inverter power, set by PV Smoothing System BESS limitations*

$P_{BESS_{lim}}$ – *BESS desired power output after power limitation*

E_{BESS} – *Accumulated energy used by PV Smoothing System*

$E_{capacity}$ – *Installed battery energy capacity*

E_{window} – *Allowable battery energy, set by PV Smoothing System BESS limitations*

SOC – BESS state of charge

t – System clock period. The PV Smoothing System runs at 1 second

4.1   First Order Low-Pass Filter

A first order low-pass filter was chosen, as was done in [12] and [14]. This filter was chosen over a moving average because the frequency-domain transfer function features less ripple at the cutoff frequency. It was chosen over a second-order filter for simplicity of the real-time system, as all three filter options produced similar smoothing results when tested against each other.

The block diagram shows transfer function for a first order low-pass filter with time constant τ. The time constant can be varied to improve the performance the filter in the presence of different weather and system conditions. The units of τ are seconds, and it represents the period of the cutoff frequency in radians. To calculate the period of the cutoff frequency in Hz, τ is multiplied by 2π. The filter characteristic is shown in the frequency domain as well as equivalently in the time domain in Figure 3 for a time constant of $\tau = 400$. The time domain characteristic is the same as the filter impulse response.
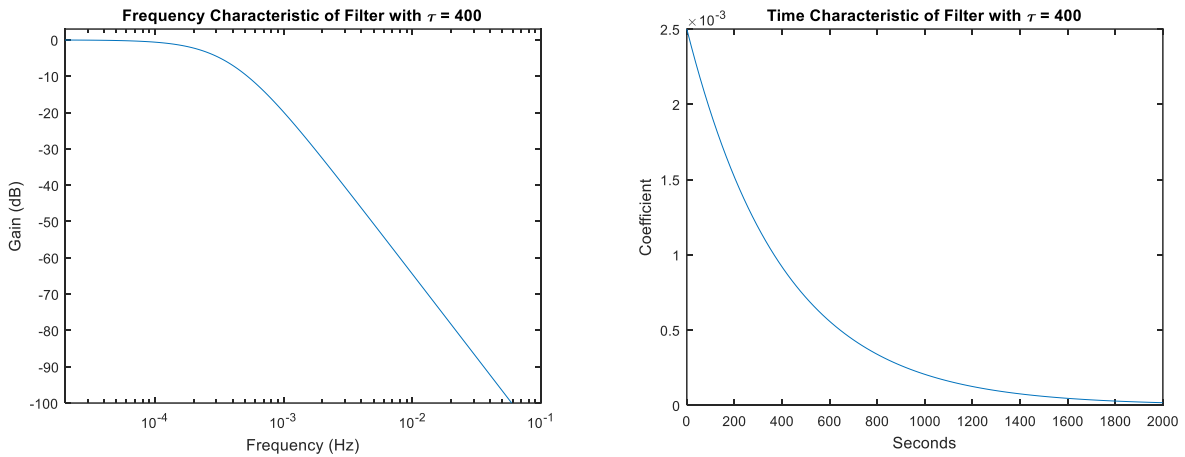
Figure 3: Frequency and Time Series Characteristic for $\tau = 400$ Filter

For the purposes of programming the filter in the VOLTTRON™ python-based framework, the filter is implemented using convolution of the time domain filter characteristic. Choosing a different time constant τ requires a new time domain characteristic to be calculated.

4.2   BESS Limitations

4.2.1 Cost of BESS Operation

One of the limitations to consider for this algorithm is the cost of dispatching the BESS unit. There are various models for determining the cost of battery cycles, several of which are detailed in [23]. The BESS in procurement for this application is of the lithium-ion chemistry.

The cycles required by the PV Smoothing System are shallow, as the goal is to remove the short term second-level oscillations. The BESS will often be charging or discharging for a matter of seconds for the purposes of smoothing. This means that should the smoothing system be the only use of the BESS without a charging or discharging bias, then the BESS will switch between the charge and discharge state quickly. Fast switching between BESS states with shallow depth of discharge has been reputed to cause the "memory effect" in nickel-based battery chemistries, which leads to nonlinear BESS dispatch behaviors. However, a similar memory effect was also identified in lithium-ion batteries in [24].

Because this memory effect issue has been identified with multiple battery chemistries, this project devised a method to prevent frequent switching between charge and discharge states with shallow depth of discharge. It is programmed as a configurable setting so that frequent state change can be permitted in the case the battery is not susceptible to the memory effect. In the solution devised for this project, BESS is held at an output bias so that the PV Smoothing System can introduce oscillations to the point of operation without crossing the zero-power threshold.

If the PV Smoothing System is the only application using the BESS, a constant bias may be held on the BESS to replicate a simple peak-shaving algorithm – discharging at a constant level during the day during high system demand while charging at night when during low demand. The bias must average to zero charge over the course of a day. It must also avoid completely charging or discharging the battery, as this results in nonlinear charge/discharge behavior.

If the PV Smoothing System is not the only application using the BESS, the BESS instructions can be coordinated with the other systems using the BESS such that the resulting bias does not cross the zero-power threshold more frequently than is necessary. This is discussed further in Section V .

4.2.2 Power and Energy Constraints

[12] and [13] include considerations for keeping the BESS within a range of SOC – done by algorithmic control and appropriate sizing, respectively. This project enforces a range of SOC by configurable parameters indicating the power and energy limits of the BESS. This is realized by constraints enforcing an adjustable limit on the percent of the BESS rated inverter output power it is allowed to use for smoothing, as well as an adjustable limit on the percent of the battery's stored energy available for smoothing.

One application of these constraints is to govern the portion of the BESS dedicated to PV smoothing. In the context of sharing the BESS, these limits prevent the PV Smoothing System from overreaching predetermined power and energy limits and negatively impacting other systems using the BESS. This is one method by which the BESS can be purposed to serve multiple applications at once. In addition, the BESS can be prevented from reaching its limits, and a range of SOC levels can be enforced.

Another application of these constraints is to investigate sizing considerations on PV Smoothing Systems. By adjusting the inverter power and battery energy of the BESS, researchers can determine the appropriate size of equipment being installed for PV smoothing. One of the goals of this project is to analyze the effect of changing these BESS parameters on PV smoothing results.

4.3 BESS Model

The team turned to a mathematical model of a lithium-ion battery as the equipment is being procured and installed at the time of writing. The model is based off of the battery model included in the Matlab-Simulink SimPowerSystems library and described in [25]. The mathematical model is implemented in its own BESS interface agent, which takes as an input the BESS instructions from both the Energy Cost Optimization and the PV Smoothing Systems, summing the two signals.

The output is the state of the battery including SOC, output power, voltage, and current. Excepting the case where the BESS is close to full charge or zero charge, the desired power generally results in an ideal output power from the BESS. The error experienced between the BESS commanded power and the BESS output grows increasingly as the unit approaches full or zero charge.

The BESS model is tuned to the same parameters as the unit to be installed. When the installation of the BESS equipment occurs, the BESS interface agent will be replaced with another interface that sums the battery instructions and communicates with the BESS unit over the VOLTTRON™ master driver.

4.4   Time Constant Selection

Altering the filter time constant τ is the most effective variable for changing effect of the smoothing system. In the ideal case, a higher time constant involves heavier use of the BESS for smoother net generation, as measured by the smoothness score. The time constant could theoretically be increased without bound until the net generation is constant throughout the day. This is not practically feasible, as it would require unrealistic demands from the BESS. Nonetheless, a larger BESS will allow more aggressive smoothing of the PV system. In this way the size of the BESS could determine the feasible severity of the smoothing filter. The inverter power and battery energy limitations on the BESS introduce further constraints to consider when selecting the best filter time constant.

The time constant selection for the PV Smoothing System is considered for two methods: a static method and adaptive method. These two approaches are studied for their effect on system performance.

Static time constant selection features one historical training period over which the best time constant is chosen. Once τ_{best} is selected, it is therefore used agnostic of seasonal, weather, or system changes. The system must be restarted if recalculating the best time constant is desired as a result of any of these situational changes. The chosen time constant is considered best for all solar and cloud cover patterns that will be experienced by the PV Smoothing System.

Adaptive time constant selection features a periodic recalculation, where the historical data considered is the duration between updates. After each update period, a new τ_{best} is selected and the First Order Low-Pass Filter is updated in real time with this new time constant. The chosen time constant is considered the best performer for the next update period, at which point it will be calculated again. Therefore, this system takes into account all changes to season, weather, and system.

As solar and cloud cover patterns change with long-term seasonal patterns as well as shorter-term weather effects, the best filter design may change as well. The necessary degree of smoothing may be different between a clear, sunny day and one with fast-changing cloud cover. Depending on the weather and climate patterns of the location, as well as how frequently the system and BESS are updated with new applications, the need for adaptively selecting the time constant periodically may be different from system to system.

4.4.1 Success Metric

In order to select the best time constant τ, there must be an objective way to quantify the smoothness of one system output over another. Several existing papers discuss smoothness criteria. [12][13][16][17] use ramping bounds on the smoothed output power to verify that the systems adhered to the desired output

goals. Similarly, [6] and [10] characterize the success of its filtered power by comparing maximum ramp rates. In addition to the ramping bounds, [13] assigns a penalty cost for power fluctuation that is proportional to the maximum ramp in a time frame, as the paper aims to optimize a combined system in terms of the total cost. [6] and [14] characterize success by determining the percent of ramps that were above a certain threshold, for example 0.05% of the rated PV array power. [26] takes a unique approach to characterizing smoothness of PV output by applying wavelet transforms to measure the breadth of the resulting spectrum.

For the purposes of time constant selection, this project requires a success metric that characterizes the relative smoothness of one curve versus another. Enforcing ramping bounds may be useful, but gauging success in this binary way does not allow fluid comparisons between filters. Using the maximum ramp rate would be a measure of how tight the ramping bounds may be set, but this limits the smoothness analysis to considering how well the largest ramp is treated, without regard to ramps that may be less severe but still negative for the system. Using wavelet transforms would isolate different frequencies of variation as the day progresses, but does not directly measure the ramping which is being minimized.

If it were determined that the system could support ramps up to a certain severity, or if a specific ramping bound were being investigated, then a good metric may be determining the percent of ramps that exceed a threshold, as was done in [6] and [14]. However, this metric does not discriminate between ramps near the threshold and ramps that severely breach the threshold. Additionally, as no ramping bound could be identified for the power system studied in this project, there is no basis for which to set this threshold.

Instead of repurposing a success metric from one of these papers for use in time constant selection, a new metric was developed. Drawing from the approach in [14], a histogram of the resultant net system power was established to quantify the occurrences of different levels of second-to-second ramping. An example of such a histogram is shown in Figure 4.
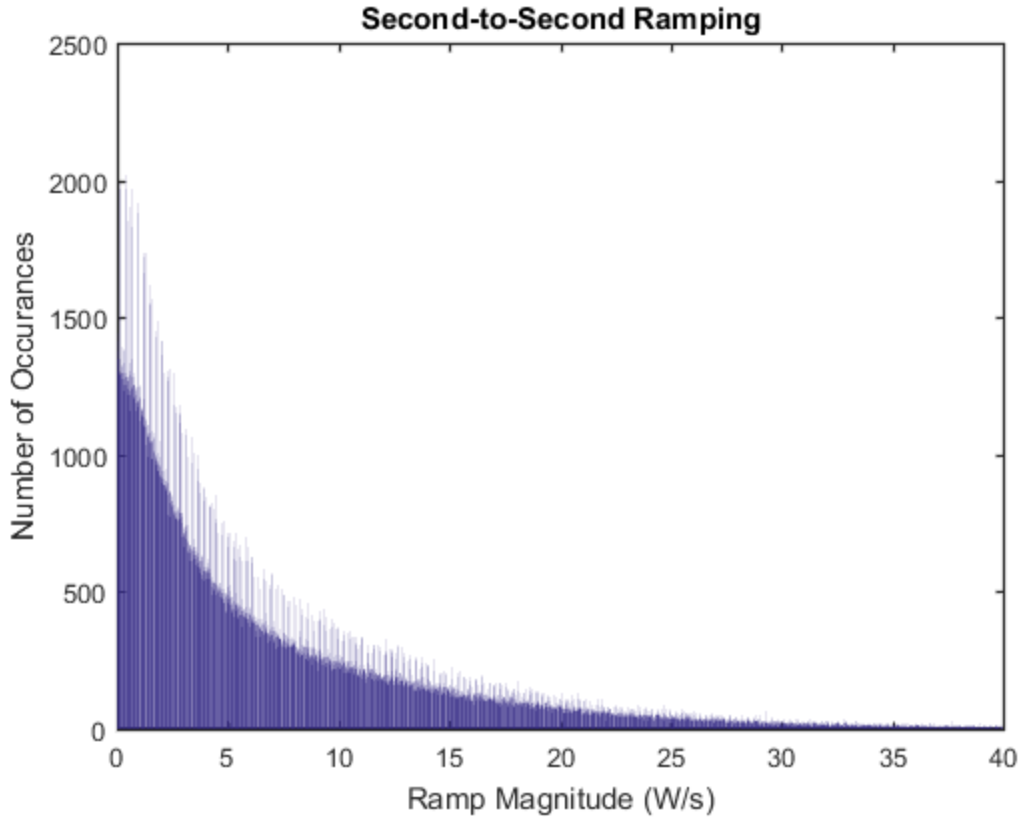
Figure 4: Histogram of Second-to-Second Ramp Rates of Raw PV Measurements

The granularity of the histogram is sufficiently small to differentiate among a broad range of system ramps. Figure 4 shows that the histogram depicts an effect where at a regular interval, a given bin has a high number of occurrences. This results in there being two curves shown in the histogram plot. This effect was deemed to be a result of the specific second-to-second ramps being artificially more commonly measured than others because of the PV meter's engineering, and was not deemed to be a significant issue in terms of generating the smoothness score.

Drawing from the cost penalty used in [13], a penalty was assigned to each second-to-second ramp in proportion to the severity of the ramp. This was done by taking each column of the histogram and multiplying it by a penalty function:

$$\boldsymbol{Score} = \sum_{i=1}^{max} \boldsymbol{H_i P_i} \qquad\qquad \textbf{13}$$

H - Set of columns in the ramping histogram

P - Penalty function

i – Histogram column index

The penalty function P increases in proportion with the severity of the ramp. The scale of this function does not matter, as it is only used for comparison. A nonlinear penalty function could be considered if higher ramps are deemed more detrimental to the system than is characterized by this equation. A step-wise penalty function could also be implemented, such that all ramps under a certain threshold have zero penalty. Appropriate definition for this function takes into account other generation on the system and any other ancillary costs involved with keeping the system flexible enough to incorporate the PV generation. For the purposes of this study and for simplicity, the penalty function is taken as the linear case:

$$P_i = i \tag{14}$$

Further research into the effect of ramping on the power system markets and stability could be performed to determine a penalty function that more accurately characterizes the cost of ramping on the power system. The product in Equation $Score = \sum_{i=1}^{max} H_i P_i$

13 is summed over a number of entries sufficient to capture more than 99.9% the ramps for a given duration.

It should be noted that while the smoothness score has no physical significance, when the penalty function is linear, the smoothness score is proportional to a measure of the total ramping that occurs on the system. With appropriate scaling, the smoothness score could represent a metric of "total second-to-second ramps." Another way to calculate the smoothness score in the linear penalty function case would be to sum up the magnitudes of each individual ramp throughout the course of smoothing.

With this smoothness score metric, a lower score indicates a smoother result. More severe ramps were penalized more than less severe ones, and all second-to-second ramps were taken into account. This solution produces a smoothness score that can be objectively compared across days, filters, and sets of parameters.

4.4.2 Choosing the Best Time Constant

The best time constant may be found for any historical set of data by running through the smoothing algorithm using the smoothing score from Equation $Score = \sum_{i=1}^{max} H_i P_i$

13 as the objective function. Running the algorithm over a range of filter time constants will result in one filter producing the lowest smoothness score: the best filter. In general, the more relaxed the constraints are on the system in terms of BESS use, the longer the duration of the best time constant will be.

It cannot be known with absolute certainty what the best time constant for a future timeframe will be, so time constant selection must either rely purely on historical data or consider forecasts. Calculating

how cloud cover forecasts impact the τ_{best} out of the scope of this project, and would rely on training a model to calculate how the most likely τ_{best} value corresponds to the actual value for different forecasts.

In order to perform time constant selection for this real-time system in the absence of forecasting, a historical time period must be chosen as the training period for finding the best filter. This variable ranges from the previous hour to many previous days, and is the basis for selecting the best time constant for future operation.

V Interface with Energy Cost Optimization System

A key aspect of this project was cooperation with a simultaneously running VOLTTRON™ research application running an energy cost optimization algorithm. This system uses solar and load forecasts to determine optimal BESS dispatch for minimizing demand charges. Because the two systems share use of the BESS, the instructions must be coordinated at every time step to ensure that BESS constraints are not breached. Important to note is that the Energy Cost Optimization System runs on a 5-minute time resolution while to the smoothing system runs at 1 second.

The Energy Cost Optimization System demands more power during an average day than the smoothing system, and requires switching between the charge and discharge regions much less frequently as well. An example of the preferred operating point (POP) as scheduled by the Energy Cost Optimization System is shown in Figure 5.
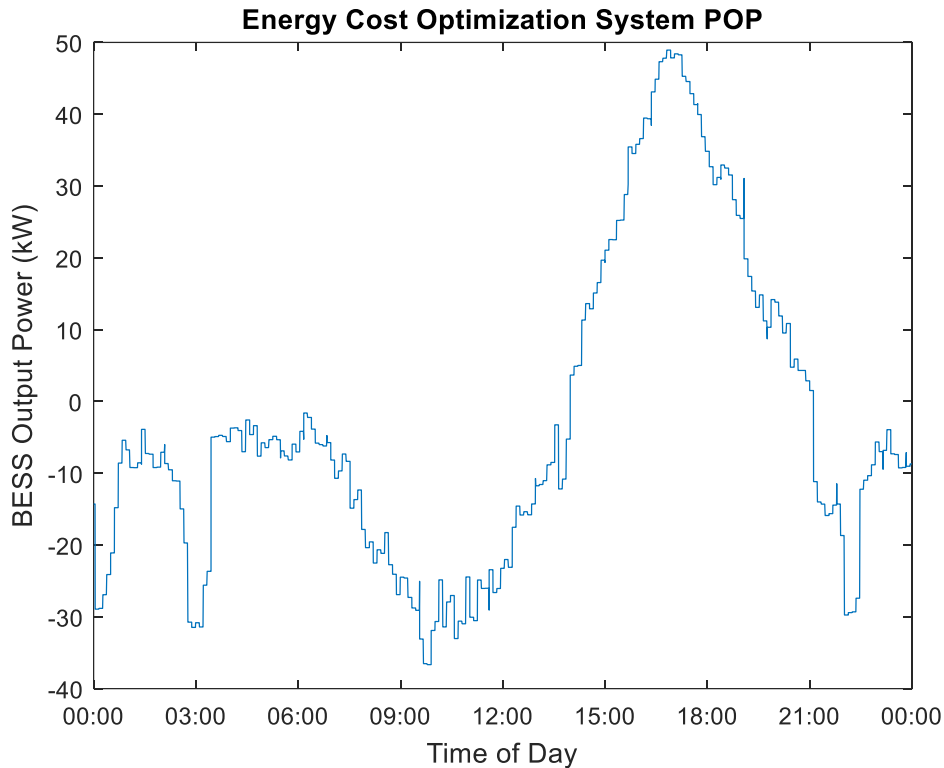
Figure 5: Preferred Operating Point of Energy Cost Optimization System

Because the Energy Cost Optimization System uses a 5-minute time step, while the PV Smoothing System runs at 1 second, the POP schedule as seen from the PV Smoothing System appears a step function, with each POP instruction is held for 300 seconds. The entire system runs on a 1-second clock, publishing metered data and sending BESS instructions, but the Energy Cost Optimization System only performs operations every 300 clock cycles. In this way, the two systems can operate at different time resolutions on the same equipment, communicating at the 1-second level.

As discussed in the context of BESS limitations in Section 4.2 , it is beneficial to certain battery chemistries to avoid switching between the charge and discharge states frequently. The optimized BESS POP schedule from the Energy Cost Optimization System changes between charge and discharge only a few times a day, as seen in Figure 4, and has an average power greater than the average power required by the PV Smoothing System.

Therefore, in order to avoid the high-frequency oscillations between the charge and discharge states, the output power for the PV Smoothing System is limited by the scheduled POP for the Energy Cost Optimization System. When the scheduled POP is close to zero-power (or also close to the maximum charge/discharge power), the PV Smoothing System cannot charge or discharge such that the net dispatch changes the state of the BESS (or exceeds the charge/discharge limit). The effect of this scheduling policy

26

is that the two systems can coexist simultaneously without overusing the BESS to the detriment of its lifetime.

VI   Photovoltaic Generation Measurements

Communication with the 35 kW PV array occurs via the PV interface agent. The agent listens for each system clock signal on the message bus, at which point it requests the VOLTTRON™ master driver agent to query the smart meter using the Modbus protocol for 1-second power generation. The agent publishes this measurement to the message bus to be utilized by both the Energy Cost systems.

The system clock is based on the VOLTTRON™ heartbeat function. The 1-second period assigned to this function has a small amount of noise. This can mean that the system will at times (on the order of 10 times per day) pull the same 1-second measurement from the smart meter on two different clock cycles, or miss one measurement.

In addition, there are instances where the Modbus query to the meter times out (on the order of 2 times per day), which can delay progress of the progress of the real-time system. In the case of a missing point, the PV interface will use the most recent successful measurement as the current measurement to enable the system to continue to run. Because the frequency of these events is so low in comparison with the number of seconds in a day, they are not seen to be an issue for operation.

Simulation analysis for this project is based on a continuous segment of 26 days of PV generation at 1 second resolution, shown in Figure 6. The data was taken between February 4th, 2017 and March 1st, 2017.
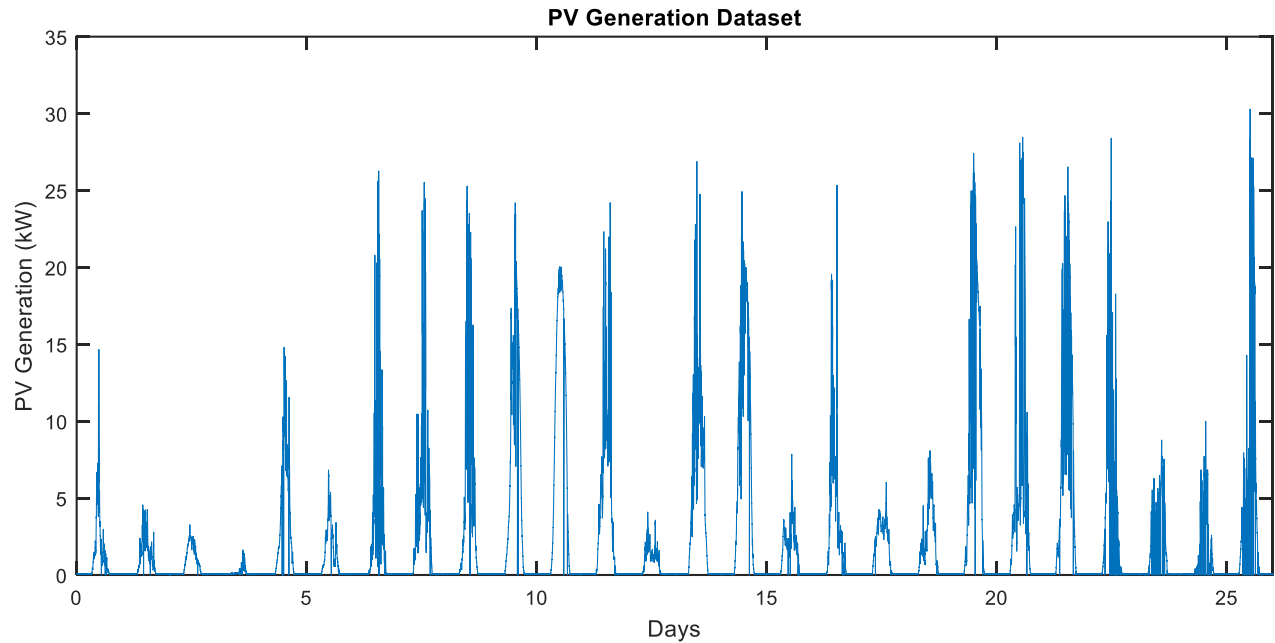
Figure 6: PV Measurements over 26 Days in February 2017

The data used for analysis show a wide variety of cloud cover conditions during one of the most overcast months of the climate in Seattle, WA. It should be mentioned that at the time of data acquisition for simulation purposes, only measurements from phase A of the PV array were available, which is equivalent to one third of the 35 kW array. In order to model the behavior of the entire array, the power output of phase A was multiplied by 3.

PV measurements were taken in real time for real-time operation of the PV Smoothing System. The results presented here for real-time operation were taken from the same 35 kW array in May, 2017. At the time of real-time operation, all three phases of the PV meter were active operating normally. Comparing the phase A-approximated measurements with actual measurements, it was determined that the phase A approximation was a good estimate for system generation and could be used for simulation analysis. This data is included as a file in the appendix.

VII   Testing and Results

The first three parts of the results section involve using the 26-day dataset for system simulation and analysis. First, the system is simulated in the unconstrained BESS case, where unlimited resources may be used for PV smoothing. Next, the effect of constraining BESS resources is analyzed. Section 7.3 discusses the process with which the filter time constant may be selected, as well as a comparison of time constant selection methods between the static and adaptive approaches.

Finally, Section 7.4 outlines real-time operation of the PV Smoothing System, demonstrating feasibility of this system in VOLTTRON and identifying the limitations of constrained BESS operation that were analyzed on the simulation dataset. Synchronization with the Energy Cost Optimization system is also shown.

7.1 Unconstrained Operation

For a given system, the time constant is the best way to modify the effectiveness of the filter. A longer time constant will incorporate more data points into the calculation, meaning that any sharp change in a data point is less likely to cause a variation in the filtered result. In this study, the time constant τ was analyzed in the range from 50 to 4800, which corresponds to a range of 314 to 30,159 seconds.

Figure 7 demonstrates the effect of various time constants on the resultant power from operation on one day, using three values of τ to show various levels of smoothing. Larger values of τ were chosen for this figure because they are the most distinguishable when viewing the day as a whole. There are no limitations placed on the BESS inverter power or battery energy apart from coordinating charge and discharge regions with the Energy Cost Optimization System.
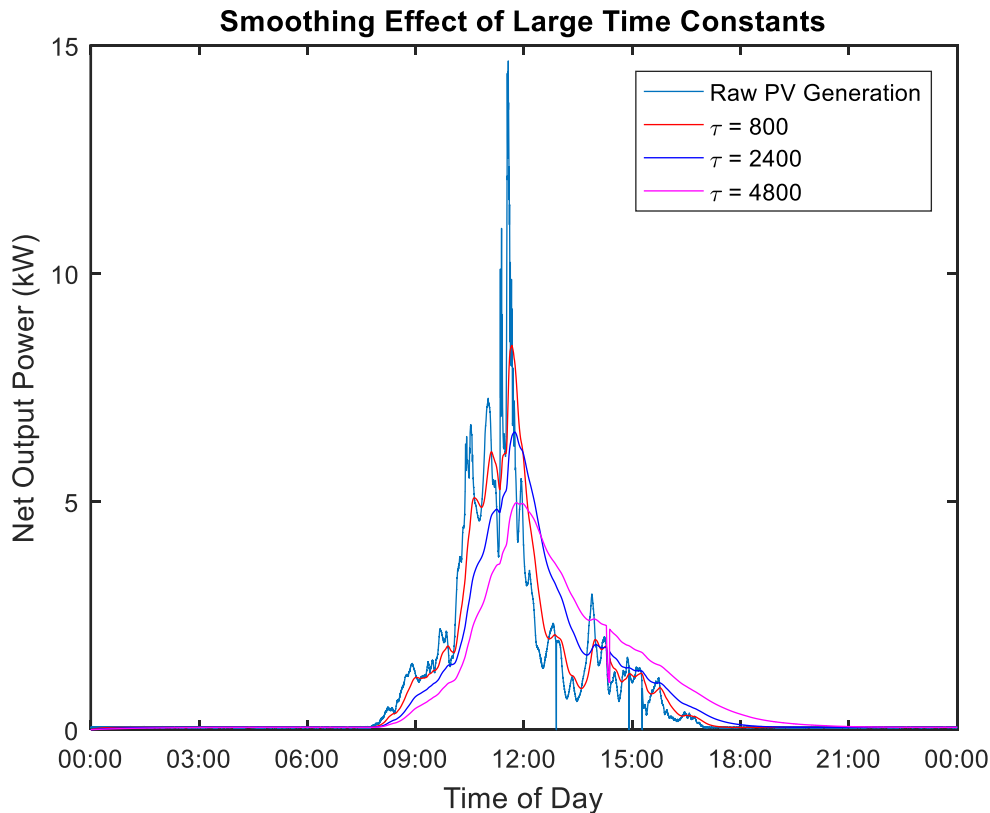
Figure 7: Smoothing on February 4th, 2017 with No Constraints, Large τ Filters

It can be seen in Figure 7 that filters featuring a higher time constant result in a smoother net power. The severe $\tau = 4800$ filter almost entirely eliminates fluctuations apart from the rising and setting of the sun. However, with a larger filter time constant, there also appears a delay in the system output. While the raw PV generation reaches its peak around 11:33 a.m., the net output from $\tau = 4800$ reaches its peak around 11:46 a.m. As the generation returns to zero at sunset, this delay is even longer. This delay results from higher time constant filters incorporating a larger number of historical points into their calculation – in the case of $\tau = 4800$, the filter considers around 24,000 data points.

As a consequence of this delay, the large time constant filters maintain a large discrepancy in power between the PV contribution and the system output, meaning the BESS needs to compensate a large sustained power to compensate. This not only means the BESS must have enough inverter capacity to meet the discrepancy, but that the BESS needs to be much larger in terms of battery energy in order to charge or discharge the required amount of energy. The energy required to maintain the large time constant filters in operation equals the integral of the difference between the PV and net generation curves at any point.

In order to view the shorter-term variations and how they are smoothed by all ranges of time constant filters, Figure 8 zooms in on a section between 9:00 and 10:00 a.m. on the same day.
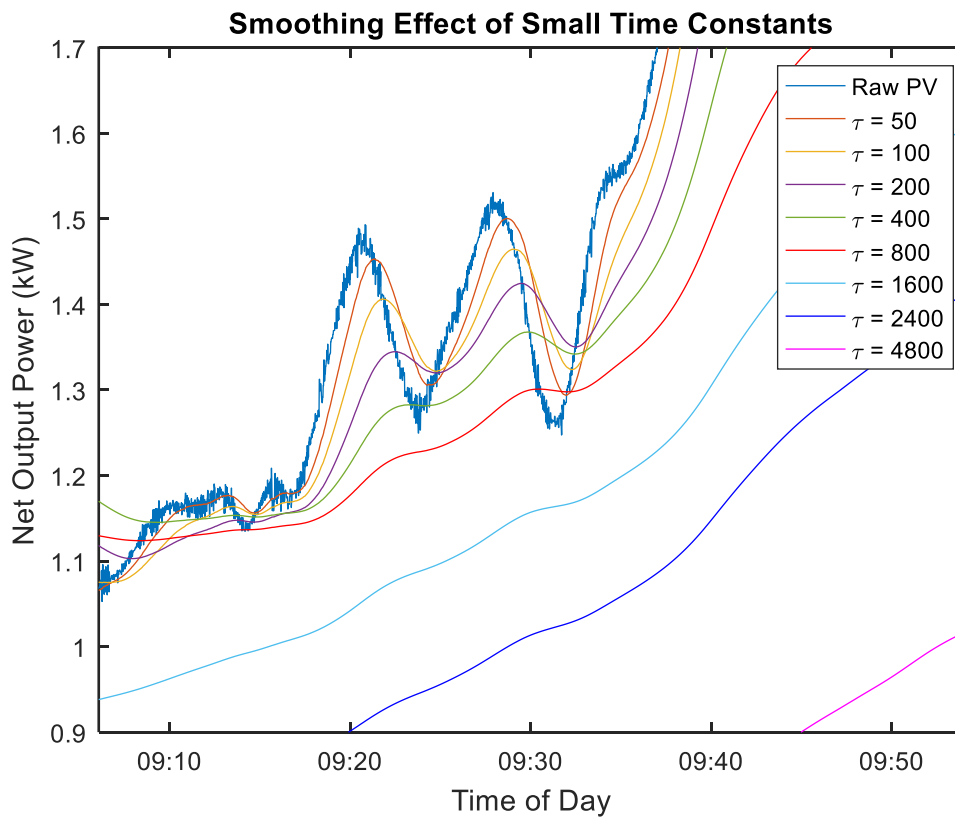
Figure 8: Smoothing on February 4th, 2017 with No Constraints, Short-Term Variations

In this figure, it can be seen that the raw PV generation features high variability on the order of seconds, and that even the lightest filter at τ = 50 eliminate the shortest-term variations. It can be seen that increasing the time constant decreases the sensitivity to fast changes in PV output, such that the net generation becomes smoother and smoother. However, the delay associated with filtering the PV generation with longer filters is also seen, with larger time constant filters rising more slowly in power to respond with the rising sun.

To quantify the extent to which each filter smooths the PV generation, the smoothing score approach is applied to the net system generation. For each filter time constant and the base case of raw PV generation, the smoothness score is calculated per Equation $Score = \sum_{i=1}^{max} H_i P_i$

13 in Table 1.

Table 1: Smoothness Score for Range of Time Constants on Unconstrained System, February 4th, 2017

Filter	Smoothness Score (Lower Score = Smoother Result)
Raw PV	527.19
τ = 50	70.23
τ = 100	59.95
τ = 200	48.11
τ = 400	36.09
τ = 800	26.04
τ = 1600	19.54
τ = 2400	17.21
τ = 4800	14.44

It can be seen from this table that the smallest filter provides a significant improvement over the raw generation. This is because the PV generation data featured very fast fluctuations due to the irregular cloud cover on this day. It can also be seen that each increase in time constant improves the smoothness. The improvements in smoothness score diminish as the time constant reaches the highest values.

7.2 Constrained Operation

To compare with the results of the previous section, the same day of solar data was analyzed in the same manner as before, only constraints on the BESS inverter power and battery energy were enforced. To illustrate a tightly constrained system where the PV Smoothing System receives only a small fraction of

BESS resources, the inverter power is constrained to 2.5 kW and the battery energy to 3.25 kWh. Figure 9 illustrates the effect these system constraints have on the PV Smoothing System on data from February 4th, 2017.
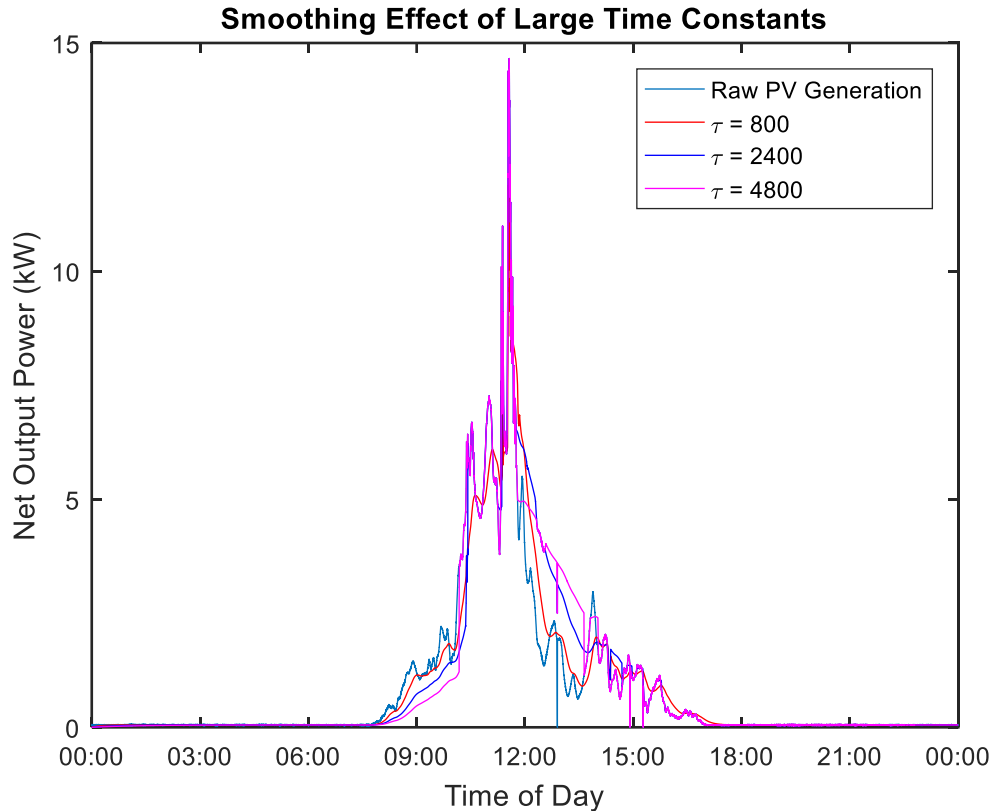
Figure 9: Smoothing on February 4th, 2017 with 2.5 kW/3.25 kWh BESS, Large τ Filters

When comparing this figure with Figure 7, it is clear that PV smoothing does not occur to the same desirable degree as when there were no constraints on the system. For example, the $\tau = 4800$ trace no longer filters the PV output to the same degree. Smoothing occurs until just past 10:00 a.m., at which point the filter stops effectively smoothing the PV generation, as the BESS has charged to the battery energy limitation. Smoothing begins again in the afternoon, only to stop once more after 2:00 p.m. when the BESS has discharged the capacity allowed by the battery energy limitation.

Figure 10 depicts a window of time between 10:00 and 11:00 a.m. where the effect of BESS constraints can be more clearly seen.
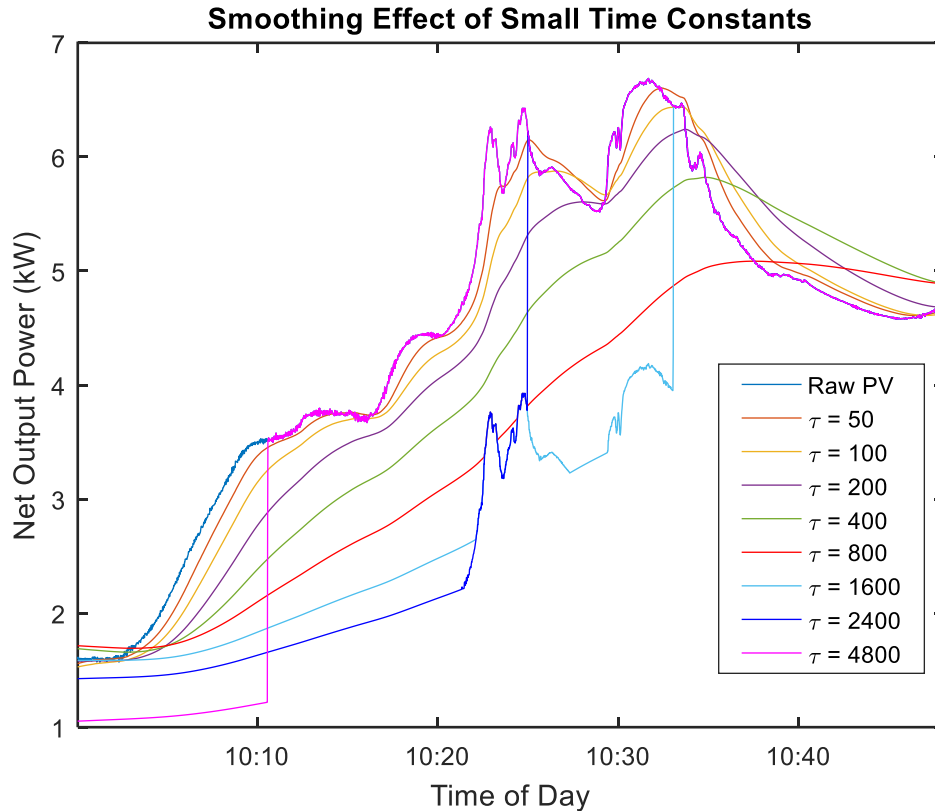
Figure 10: Smoothing on February 4th, 2017 with 2.5 kW/3.25 kWh BESS, Visible Constraints

With the limited BESS resources in this scenario, the most aggressive $\tau = 4800$ filter is the first to reach the constraint. When the BESS can no longer charge in order to absorb variations in PV generation, the system is at the mercy of the short-term variations from the raw PV output. After the $\tau = 4800$ filter reaches its capacity, so too do the $\tau = 2400$ and $\tau = 1600$ filters. These filters use their allotted battery energy at a pace corresponding to the aggressiveness of the filter, each in turn reverting to the unsmoothed signal as the capacity is exhausted.

Also notable is that around 10:20 a.m., the limitation on inverter power is expressed with filters ranging from $\tau = 800$ to $\tau = 2400$. The PV generation signal rises quickly, and soon leaves the operable region of allowed inverter power for smoothing. Because the limitation for the PV Smoothing System's share of the inverter is set to 2.5 kW, the desired smoothing setpoint cannot be further than 2.5 kW above or below the raw PV generation. This is comparable to using a 2.5 kW inverter for PV smoothing. This also sets a minimum on where the PV smoothing setpoint can be located, and this is expressed as an image of the raw PV curve translated -2.5 kW. When the net system output intersects this image, it must follow the trace until the desired output is within the inverter range.

The power and energy limitations of the BESS are more clearly depicted in Figure 11, which shows the state of these resources throughout the operation of the PV Smoothing System on this day. The resources depicted represent the portion of the BESS devoted to PV smoothing, and not the definitive state of the BESS across all applications.

Inverter Power During PV Smoothing

Battery Energy During PV Smoothing
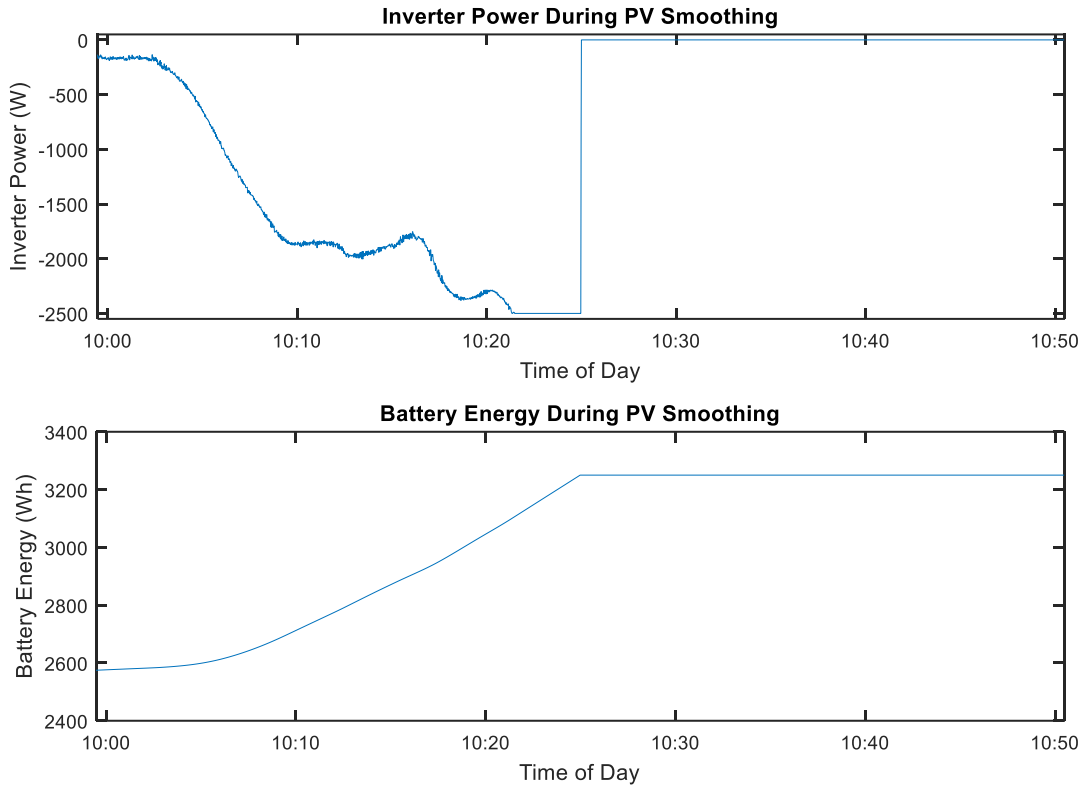
Figure 11: BESS Power and Energy during PV Smoothing on Constrained System, February 4th, 2017

As can be seen in Figure 11, the inverter output power is limited to ±2.5 kW. When more than this amount is requested of the BESS, as occurs around 10:21 a.m., the contribution is limited to the maximum output.

The BESS energy starts the day at 50 percent capacity charged. As PV generation begins to rise, the system begins to charge and the battery energy increases. Once the entire battery capacity permitted by the constraints has been charged, as occurs at around 10:25 a.m., the BESS rests at the capacity of 3.25 kWh. At this point, the BESS can no longer charge, and the power output reverts to zero. This means that the BESS can no longer assist in PV smoothing until a discharge instruction is called.

Table 2 shows the smoothness scores corresponding to the filters which were run on this day's PV generation data with the constraints added.

34

Table 2: Smoothness Score for Range of Time Constants on Constrained System, February 4th, 2017

Filter	Smoothness Score (Lower Score = Smoother Result)
Raw PV	527.19
$\tau = 50$	75.83
$\tau = 100$	75.61
$\tau = 200$	72.64
$\tau = 400$	67.28
$\tau = 800$	67.21
$\tau = 1600$	115.76
$\tau = 2400$	198.57
$\tau = 4800$	298.89

With BESS restrictions enabled at this level, the limitations on BESS usage become apparent at higher time constants. While the lower time constants retain the same smoothness score as they had in the unrestricted case, the higher time constants exhibit a greater smoothness score, representing less desirable outcomes.

This is evidence that higher time constant filters are more demanding of the battery BESS. These stronger filters are less susceptible to large, fast changes in solar and therefore require more power from the inverter to counteract these patterns. If the desired BESS contribution is greater than the pre-allocated share of inverter power, it will not be able to perform smoothing and be susceptible to short-term variations.

Because of the time-shifting effect of higher filters as described regarding Figure 7, the sustained differences between desired net generation and PV generation require large sums of energy from the battery. When the limit is reached, the BESS may no longer perform smoothing functions in whatever state it has saturated (charge or discharge). This results in a severely penalized smoothness score, both for the initial jump between the desired curve and the raw PV curve, and for mirroring the raw PV output for a duration.

Table 2 therefore shows the importance of selecting the correct time constant, as choosing a time constant ill-suited to the system could result in sub-optimal smoothing performance. The best time constant can perform an order of magnitude better than the worst time constant, as judged by the smoothness score.

7.3 Time Constant Selection Analysis

The best choice for filter time constant depends on many factors: the sun and weather patterns of the region and time of year, the size of the battery, and the limitations placed on the use of the battery by the PV Smoothing System. In general, more available output power and battery energy from the BESS for PV smoothing results in a larger τ_{best}.

For the data discussed in the previous section from February 4th, 2017, the best time constant depends on the constraints placed on BESS usage. In the unconstrained case, the $\tau_{best} = 4800$, and would theoretically increase to infinity if such long filters were considered in this study. However, once the BESS contribution is constrained to 2.5 kW/3.25 kWh, $\tau_{best} = 800$. This shows that the best choice of filter depends on the contribution of the BESS to PV smoothing.

τ_{best} was determined for each day in the dataset under unconstrained conditions as well as constrained ones. The result is shown in Table 3.

Table 3: Best Time Constant for Each Day in PV Dataset

Day	Unconstrained τ_{best}	5 kW/6.5 kWh τ_{best}	2.5 kW/3.25 kWh τ_{best}
1	4800	1600	800
2	4800	2400	1600
3	4800	4800	2400
4	4800	4800	4800
5	4800	800	400
6	4800	2400	800
7	4800	100	50
8	4800	400	200
9	4800	400	200
10	4800	400	200
11	800	400	200
12	4800	400	50
13	4800	4800	2400
14	4800	800	50
15	4800	400	200
16	4800	2400	800
17	4800	400	100
18	4800	2400	800
19	4800	1600	800
20	4800	400	100
21	4800	200	100
22	4800	400	50
23	4800	400	200
24	4800	1600	400
25	4800	1600	800
26	4800	800	50

It can be seen from Table 3 that with one exception (Day = 11, February 14th, 2017), the unconstrained system operates best when using the longest time constant studied in this project, $\tau = 4800$. This exception on Day 11 is a result of a data acquisition issue where the PV meter read 0 watts for a duration of around a minute and a half, distorting the results.

In the constrained 2.5 kW/3.25 kWh case, the best time constant changes almost every day. This is due to the high variability in PV generation from day to day, as shown in Figure 6. Not only does the magnitude of sun change from day to day, but the variability of cloud cover does as will. Additionally, the highly constrained case of 2.5 kW/3.25 kWh provides a very tight band of operation, which makes τ_{best} sensitive to these changes. It can be seen in Table 3 that in the less constrained 5 kW/6.5 kWh case, the best time constant is still highly variable but is slightly less volatile than when the constraints are tighter.

It can therefore be shown that the best time constant for each day depends highly on the solar patterns of the day as well as BESS constraints. To further illustrate the impact of BESS constraints on filter performance, the system was analyzed for a range of BESS constraints over the entire 26-day dataset. Table 4 and Figure 12 depict the filter performance in terms of its smoothness score over the full dataset, with the assumption that the best filter is predicted and chosen for each individual day. This represents the ideal best case scenario for selecting the time constant.

Table 4: Smoothness Score versus BESS limitations over 26 Days for Ideal Case

Ideal Smoothness Score		Battery Energy (kWh)							
		0.65	1.625	3.25	6.5	13	19.5	26	325
Inverter Power (kW)	0.5	10,858	10,784	10,784	10,784	10,784	10,784	10,784	10,784
	2.5	7,391	7,008	6,914	6,873	6,866	6,866	6,866	6,866
	5	5,633	4,956	4,638	4,481	4,426	4,416	4,416	4,416
	7.5	4,865	3,993	3,454	3,159	3,047	3,008	3,002	3,002
	10	4,676	3,635	2,919	2,454	2,259	2,191	2,162	2,162
	100	4,608	3,461	2,571	1,900	1,421	1,172	1,069	911
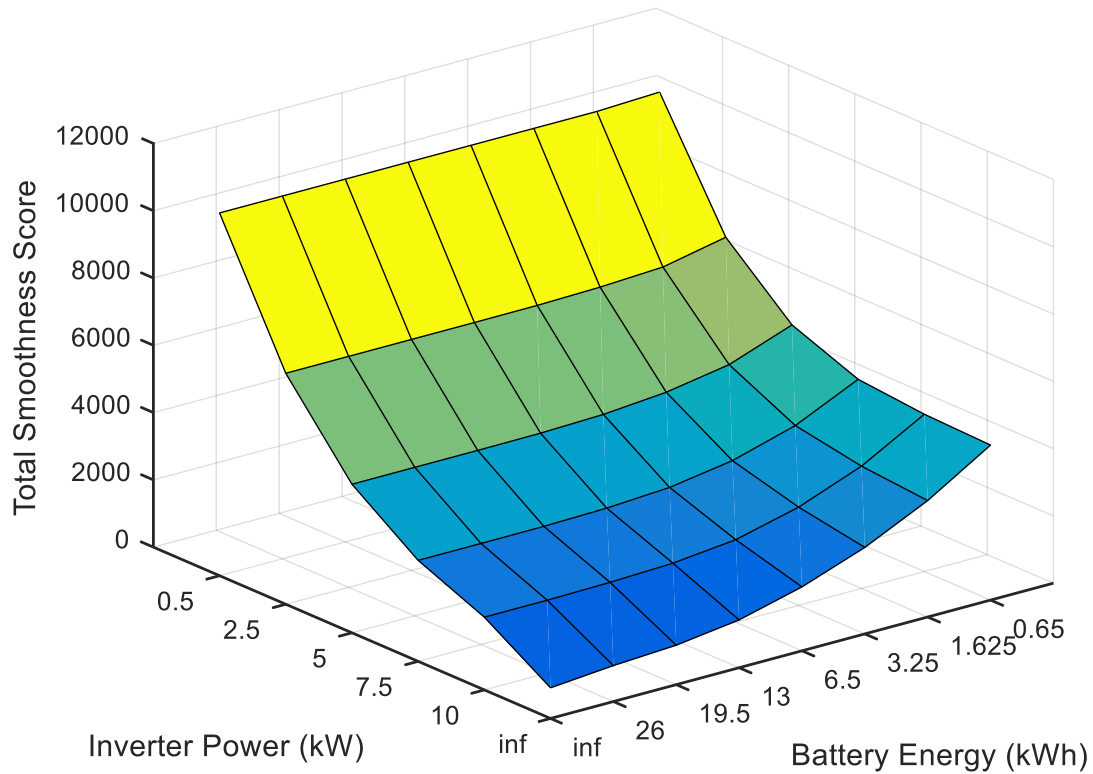
Figure 12: Smoothness Score versus BESS limitations over 26 Days for Ideal Case

inf – unconstrained parameter

For comparison, the smoothness score for 26 days of raw PV measurements is 26,101.

The first conclusion to draw from these results is that both inverter power and battery energy parameters individually have an effect on the best performance of the PV Smoothing System. It can be seen that smoothness score decreases as either parameter increases.

The exception to this rule is that increasing battery energy after a certain point will no longer benefit the performance of the system. The maximum amount of battery energy that provides smoothing benefits depends on the amount of power available to the system. This is intuitive, as increasing the power available increases the potential aggressiveness of the filter, but aggressive filter also builds a large energy imbalance that must be supported by a large battery energy. Figure 13 further illustrates this by translating the surface plot to a line graph where the inverter power is held constant. It focuses on battery energy levels under 26 kWh to depict the shape of the traces.
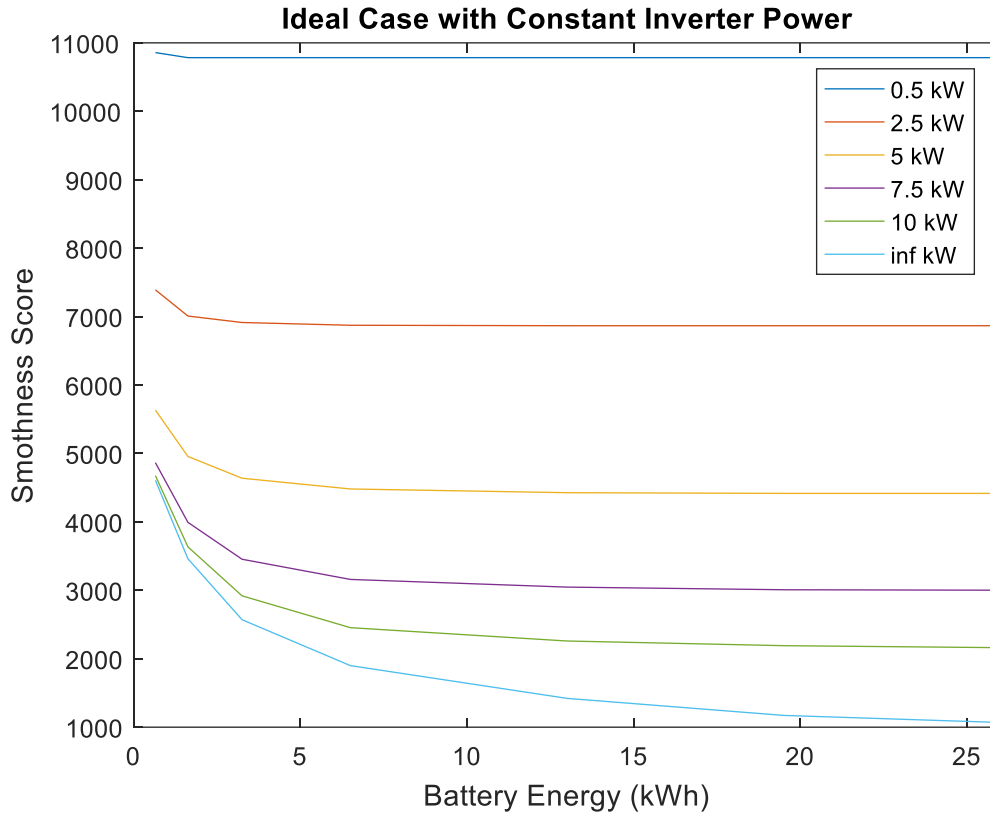
Figure 13: Smoothness Score versus Battery Energy, with Inverter Power Held Constant, Ideal Case

From this figure, it is clear that after a certain battery capacity, increased energy does not help PV smoothing unless the inverter is also augmented.

Increasing the inverter power improves the smoothness score regardless of the battery energy parameter. The improvements in score do diminish with increasing inverter size, and likely would continue past 100 kW if such inverter sizes were studied. Theoretically, the smoothness score could reduce to zero with a large enough BESS and a filter with a time constant greater than an entire day's worth of data –this would equate to constant power generation throughout the day.

In the absence of forecasting, this project relies on historical data to serve as a predictor for appropriate PV filters in the future. Two different sets of methods for selecting the filter time constant are analyzed in this study: a static method and an adaptive method.

7.3.1 Static Time Constant Selection

In static time constant selection, one characteristic time constant is calculated to minimize the smoothness score across all days. The best time constant is not always appropriate for each individual day,

but rather would maximize smoothing for as many days as possible while suffering the variations where the time constant does not suit the solar and cloud cover patterns of the day.

To explore time constant selection using static methods τ_{best} for the entire dataset was calculated based on a historical period for a variable number of days. The historical period must consist of at least one day because training performed on less than a day of data may not take into account phenomena that occur throughout the day. Analysis was done in order to determine how many days of historical data were required to make an accurate prediction of the best time constant for the 26-day period.

The results of this analysis on the 2.5 kW/3.25 kWh constrained case are shown in Table 5. Based on each historical period length, the value of τ_{best} which represents the lowest smoothness score over the entire dataset duration is calculated. The column entitled "26-day Smoothness Score" totals the smoothness scores for the entire dataset corresponding to these time constants. Finally, these scores are compared to the "Ideal Case" where the best time constant is chosen for each individual day (from Table 4), and the smoothness score of the raw PV data generation measurements.

Table 5: Static Time Constant Historical Period Length Analysis for 2.5 kW/3.25 kWh

Historical Period Length	τ_{best}	26-day Smoothness Score
1 day	50	7,482
2 days	800	8,640
3 days	800	8,640
4 days	800	8,640
5 days	400	7,628
6 days	400	7,628
7 days	200	7,230
8 days	200	7,230
9 days	200	7,230
10 days	200	7,230
Entire Dataset	200	7,230
Ideal Case	-	6,914
Raw PV	-	26,101

For context, the smoothness scores resulting from all static time constants are shown in Figure 14.
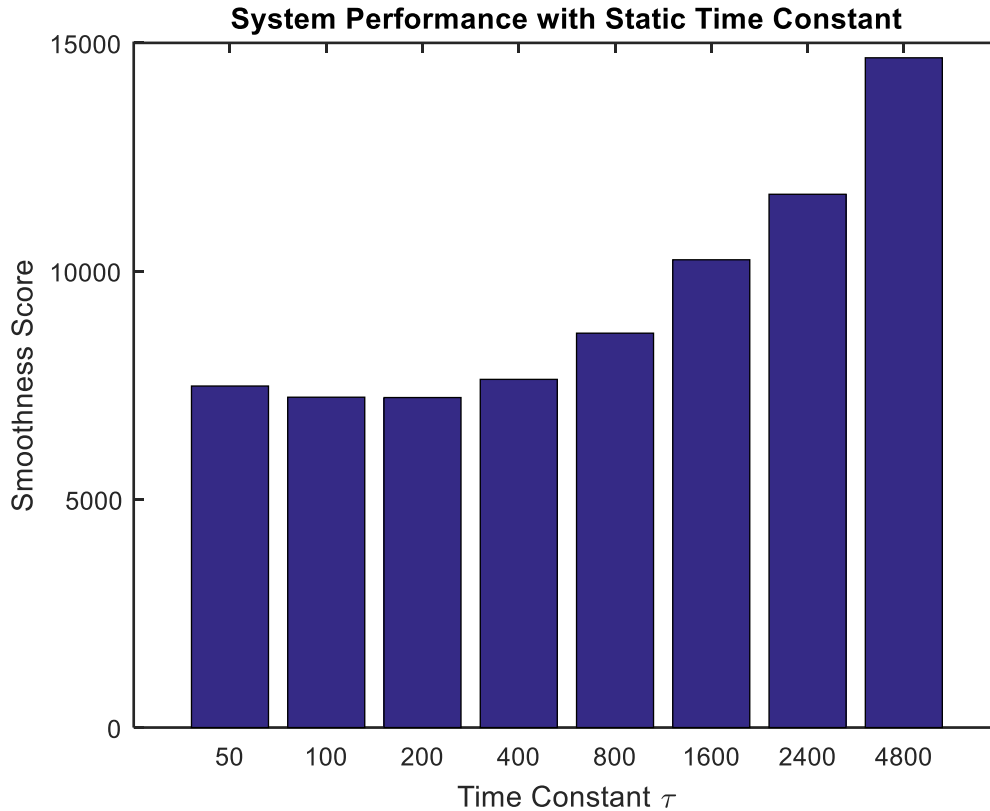
Figure 14: Smoothing Performance over 26 Days, 2.5 kW/3.25 kWh, Static Time Constant

It can be seen that with this 26-day dataset and constraints set to 2.5 kW/3.25 kWh, it takes at least 7 days of training with historical data to be able to correctly predict the best time constant of the entire dataset, $\tau_{best} = 200$. The achieved smoothness score of 7,230 for the 26-day duration approaches the ideal case of 6,914 from Table 4.

To expand this analysis, the system was analyzed to determine the amount of historical data required to make an accurate calculation of the best time constant for the entire dataset for each different configuration of BESS constraint parameters. The result is shown in Table 6.

Table 6: Length of Historical Period Required to Characterize Static τ_{best}

Length of Dataset (Days)		Battery Energy (kWh)							
		0.65	1.625	3.25	6.5	13	19.5	26	325
Inverter Power (kW)	0.5	7	7	7	7	7	7	7	7
	2.5	22	11	7	7	7	7	7	7
	5	7	5	7	10	10	10	10	10
	7.5	7	5	11	7	15	15	15	15

10	7	5	2	7	8	13	13	13
100	8	5	2	11	11	10	7	2

It can be seen that there is no obvious pattern to relate BESS parameters to the required length of the historical dataset. While the most common required length of the historical dataset is 7 days, there are many configurations in which a dataset of 7 days is not sufficient to make a judgement on the best static time constant of the system. A historical period of 15 days allows enough data to calculate the best time constant of all but one BESS parameter configuration.

Assuming τ_{best} is chosen prior to the beginning of PV smoothing on the 26-day dataset, the performance of the system can be quantified. Table 7 shows the performance of the PV Smoothing System using the best static time constant over the entire 26-day dataset and under each BESS parameter configuration. Figure 15 shows the smoothness scores plotted on a surface for comparison

Table 7: Smoothness Score and τ_{best} versus BESS limitations over 26 Days for Static Time Constant Selection Method

			Battery Energy (kWh)							
			0.65	1.625	3.25	6.5	13	19.5	26	325
Inverter Power (kW)	0.5	τ_{best}	50	50	50	50	50	50	50	50
		Smoothness Score	10,934	10,871	10,871	10,871	10,871	10,871	10,871	10,871
	2.5	τ_{best}	50	100	200	200	200	200	200	200
		Smoothness Score	7,648	7,237	7,230	7,230	7,230	7,230	7,230	7,230
	5	τ_{best}	100	200	200	400	400	400	400	400
		Smoothness Score	5,788	5,235	4,845	4,738	4,738	4,738	4,738	4,738
	7.5	τ_{best}	100	200	200	400	800	800	800	800
		Smoothness Score	5,013	4,246	3,737	3,344	3,284	3,284	3,284	3,284
	10	τ_{best}	100	200	400	400	800	1600	1600	1600
		Smoothness Score	4,827	3,862	3,187	2,664	2,408	2,345	2,345	2,345
	100	τ_{best}	100	200	400	400	800	1600	2400	4800

		Smoothness Score	4,770	3,693	2,777	2,198	1,651	1,286	1,122	918
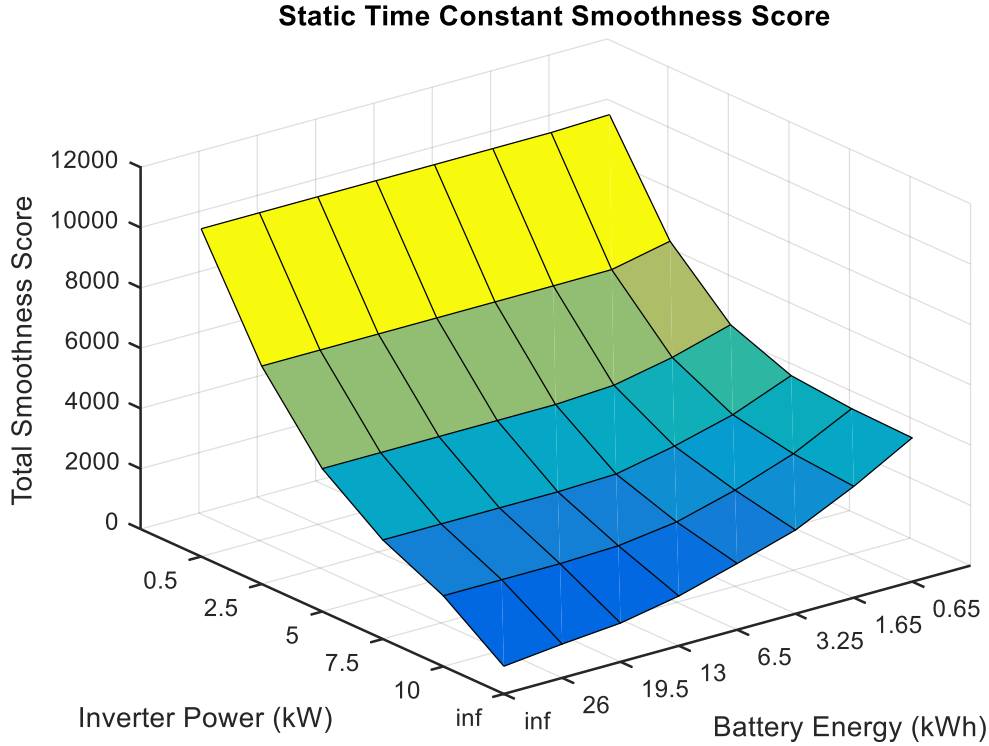
Figure 15: Smoothness Score versus BESS limitations over 26 Days for Static Time Constant Selection Method

It can be seen from the table and figure that the effect of BESS parameters on the smoothness score is similar to the ideal case shown in Figure 12. However, using a static time constant never reaches the same level of performance as the ideal case, because many days' worth of PV data are smoothed with suboptimal filters.

Studying the performance of this time constant selection method versus the ideal case is important for evaluating the success of this method. To visualize this, the percent error between the smoothness score for the best static time constant and the ideal case is shown for each BESS parameter configuration in Table 8. The percent error represents how much higher the smoothness score for the static method is.

Table 8: Static Time Constant Selection Method Percent Error

Percent Error (%)		Battery Energy (kWh)							
		0.65	1.625	3.25	6.5	13	19.5	26	325
Inverter Power (kW)	0.5	0.70	0.81	0.81	0.81	0.81	0.81	0.81	0.81
	2.5	3.48	3.27	4.57	5.19	5.29	5.29	5.29	5.29
	5	2.74	5.62	4.47	5.75	7.05	7.29	7.29	7.29
	7.5	3.03	6.32	8.21	5.84	7.78	9.17	9.41	9.41
	10	3.22	6.25	9.16	8.56	6.56	7.00	8.44	8.44
	100	3.53	6.71	8.05	15.70	16.21	9.74	5.01	0.84

The percent error for adaptive time constant selection with this distribution of parameters ranges from 1.35% to 18.86%. Table 9 shows the mean and variance of this percent error using the best static time constant, as well as using the different time constants period across all parameters.

Table 9: Mean and Variance of Percent Error across BESS Constraint Parameters, Static Time Constant Selection Method

Static Time Constant	Mean Percent Error	Variance
50	75.62%	11891%
100	46.08%	5652%
200	27.91%	2199%
400	21.67%	669.4%
800	30.08%	467%
1600	53.95%	1655%
2400	81.83%	3813%
4800	163.13%	13250%
τ_{best}	5.71%	12.53%
Raw PV	408.29%	-

7.3.2 Adaptive Time Constant Selection

In the adaptive approach to time constant selection, the time constant is recalculated on a rolling basis. Whereas in the static method the time constant is calculated once using a set of historical data for calibration, in the adaptive method the time constant is calculated periodically, where the period is the duration of the historical calibration data. The purpose for using an adaptive algorithm is to maintain

optimal operation through changes in solar and cloud patterns, as well as through changes in the system that may alter the BESS constraints assigned to PV smoothing.

This method introduces another variable to the system, the update period, which corresponds to the duration between time constant updates, as well as the length of historical data used for each update. For this study, this update period is analyzed on a range from 1 hour to 1 week.

To demonstrate the effect of altering the update period within the course of a day, Figure 16 demonstrates a range of update periods applied to the data from February 4th, 2017. The constraints placed on the BESS were 2.5 kW/3.25 kWh. The filter is initialized with a time constant of $\tau = 800$ for all cases, as this was calculated as the best time constant for the day as a whole.
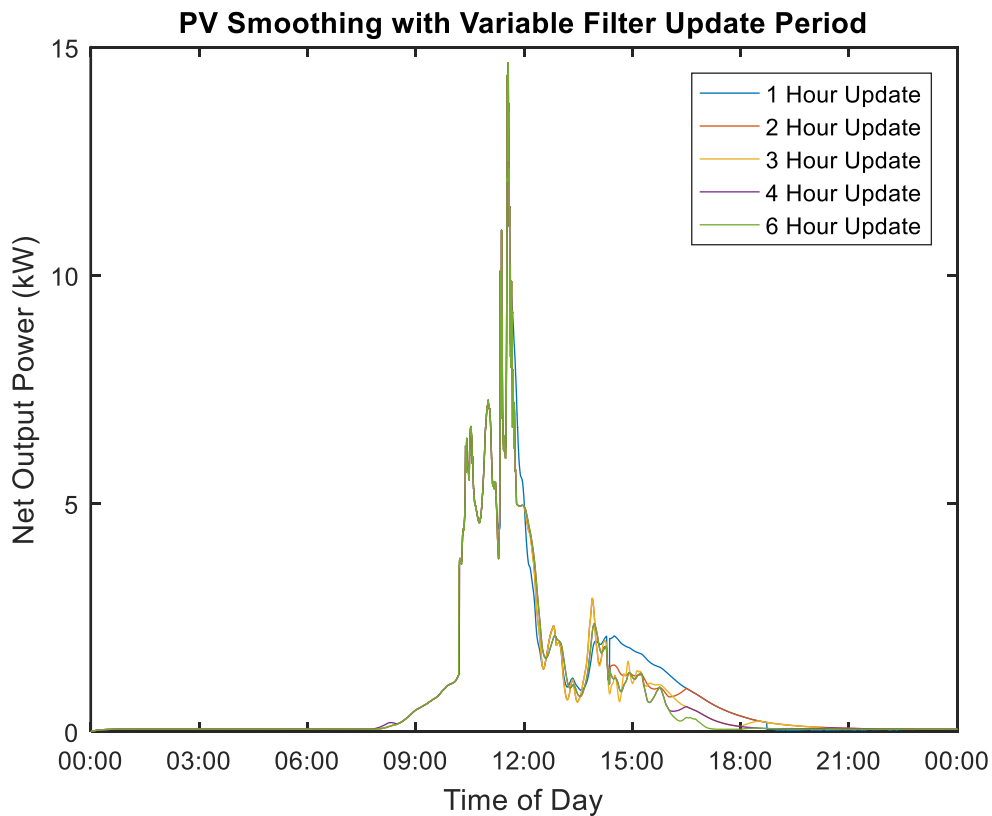
Figure 16: Adaptive Time Constant Selection with Varied Update Period, February 4th, 2017

Figure 16 shows that the systems begin the day with the same time constant though in the afternoon the different update periods have caused them to diverge. This afternoon period is shown in more detail in Figure 17.
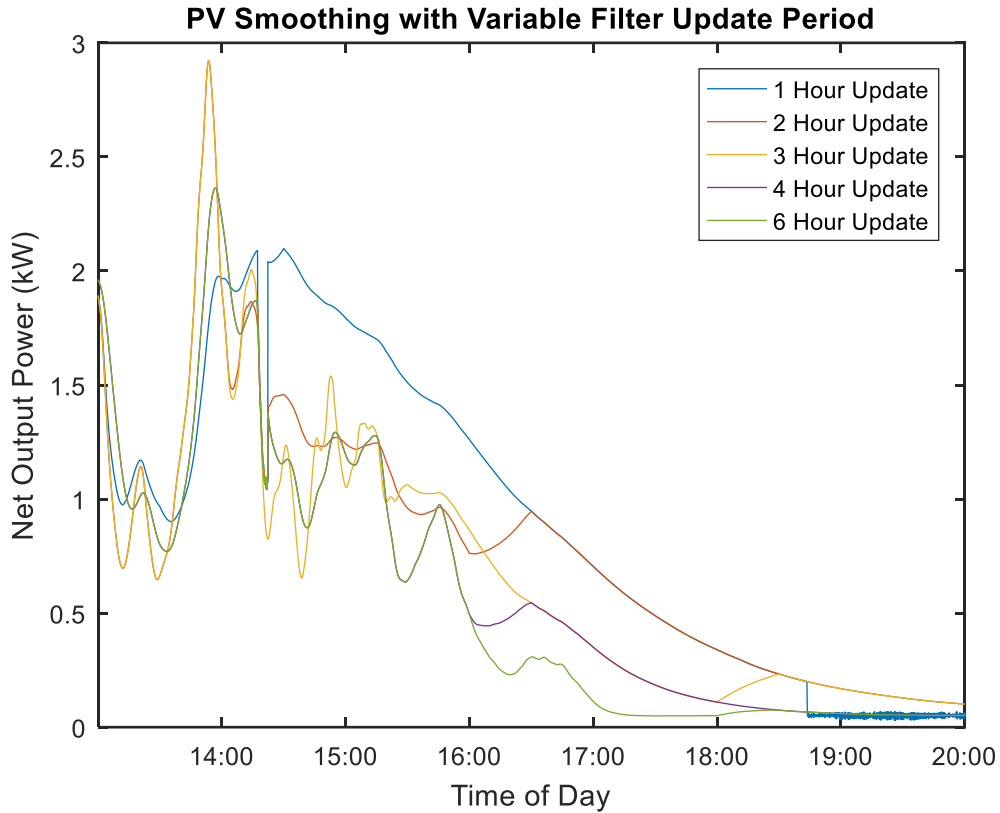
Figure 17: Time Constant Update Sequence, February 4th, 2017

Several changes in time constant can be seen from this figure. Each transition between time constants is spread out over half an hour such that the second-to-second ramps are limited. If there was no transition time, the change in time constant would spark an instantaneous ramp from one curve to another and a correspondingly undesirable impact on the smoothness score. However, even with a transition period the transitions between time constant curves can increase the resulting smoothness score.

It can be seen that there are three time constants being used by the different systems in the late afternoon. These correspond to $\tau = 400$, $\tau = 2400$, and $\tau = 4800$, with the lower time constants returning to zero generation earlier in the evening. At 4:00 p.m., it can be seen that the system with a 2-hour update period transitions from $\tau = 2400$ to $\tau = 4800$, and the system with a 4-hour update transitions from $\tau = 400$ to $\tau = 2400$. These transitions are outlined in Table 10.

Table 10: Time Constant Update Sequence, February 4th, 2017

	Time Constant Update				
Time of Day	1-Hour Update	2-Hour Update	3-Hour Update	4-Hour Update	6-Hour Update
5:00 a.m.	800	800	800	800	800

6:00 a.m.	4800	4800	4800	-	4800
7:00 a.m.	4800	-	-	-	-
8:00 a.m.	4800	4800	-	4800	-
9:00 a.m.	4800	-	4800	-	-
10:00 a.m.	4800	4800	-	-	-
11:00 a.m.	400	-	-	-	-
12:00 p.m.	50	50	50	400	400
1:00 p.m.	800	-	-	-	-
2:00 p.m.	4800	1600	-	-	-
3:00 p.m.	4800	-	2400	-	-
4:00 p.m.	4800	4800	-	2400	-
5:00 p.m.	4800	-	-	-	-
6:00 p.m.	4800	4800	4800	-	2400
7:00 p.m.	4800	-	-	-	-
8:00 p.m.	4800	4800	-	4800	-

The different values of time constant update period result in smoothness scores as shown in Table 11.

Table 11: Smoothness Scores for Adaptive Filtering with Varied Update Period, February 4th, 2017

Update Period (Hours)	Smoothness Score (Lower Score = Smoother Result)
1	164.94
2	141.61
3	142.31
4	139.22
6	139.48
Ideal Static ($\tau = 800$)	67.21
Raw PV	527.19

Table 11 shows that the best period for updating the time constant is 4 hours, though the smoothness scores for all update periods greater than 1 hour are within 3 points of each other. Most notably, these methods fall far short of the score achieved by using $\tau_{best} = 800$.

This is because, while $\tau = 800$ was assigned at the start of the day, the early hours of the day featured low PV generation which was best smoothed with the aggressive $\tau = 4800$ filter without hitting the BESS constraints. As the day progresses, the magnitude of PV increases, as does the potential for variability. This means that the system is more likely to reach its BESS constraints.

Looking at the 1-hour update column of the table, it can be seen that the calculated τ_{best} values in the middle of the day when the sun is strongest are the lowest. Within the space of 2 hours, the 1-hour τ_{best} drops from 4800 to 50. Further, because it is known that the best time constant for the entire day as a whole is $\tau = 800$ (from Table 3), it can be inferred that the magnitude of variations experienced during this three-hour period is large enough to bring the average τ_{best} for the entire day from 4800 to 800, even though the most common 1-hour $\tau_{best\ is\ 4800}$. This is confirmed when looking at Figure 16, as the time period between 10:00 a.m. and 1:00 p.m. indeed depicts the highest magnitude PV generation and variation of the day.

This is evidence that the PV generation in the morning and evening do not always feature the same variation patterns as mid-day generation. Filter time constants calculated based on morning data may not be appropriate for mid-day operation, as the range of variability increases with the magnitude of generation. Therefore, the update period was considered to have a minimum of one day so that PV patterns over the entire day can be considered at once.

To analyze filter update periods on the order of days, the system was run for the entire 26-day dataset. Update periods were studied in the range from 1 to 7 days. The time constant was once again initialized with $\tau = 800$. This filter was maintained throughout the duration of the first update period, at which point the accumulated data was used to recalculate the time constant for the next period. Table 12 shows the results for the 26-day dataset using update periods from 1 to 7 days for the constrained case of 2.5 kW/3.25 kWh. These results are compared against the ideal case where the best time constant is chosen for each day.

Table 12: PV Smoothing Performance over 26 Days, 2.5 kW/3.25 kWh, Variable Update Period

Update Period (Days)	Smoothness Score
1	8,321
2	7,486
3	7,275
4	7,430
5	7,281
6	7,362
7	7,245

| Ideal Case	6,914
Raw PV	26,101

These results show that smoothness score tends to improve as more days are considered in each recalculation, with a 7-day update period yielding the best results. This trend would likely continue as the update period increases beyond 7 days, though the benefit of incorporating more days into the calculation diminishes as the update period increases.

To expand this study to all ranges of BESS parameters analyzed in this project, Table 13 lists the best update periods and their corresponding smoothness scores for each combination of constraints. These results are also shown in Figure 18.

Table 13: Smoothness Score and Best Update Period versus BESS limitations over 26 Days for Adaptive Time Constant Selection Method

			Battery Energy (kWh)							
			0.65	1.625	3.25	6.5	13	19.5	26	325
Inverter Power (kW)	0.5	Best Update Period	3	3	3	3	3	3	3	3
		Smoothness Score	11,004	10,934	10,934	10,934	10,934	10,934	10,934	10,934
	2.5	Best Update Period	2	3	7	7	7	7	7	7
		Smoothness Score	7,751	7,204	7,245	7,245	7,245	7,245	7,245	7,245
	5	Best Update Period	4	3	5	7	7	7	7	7
		Smoothness Score	5,874	5,261	4,860	4,775	4,842	4,842	4,842	4,842
	7.5	Best Update Period	4	6	7	7	7	7	7	7
		Smoothness Score	5,094	4,247	3,716	3,344	3,280	3,280	3,280	3,280
	10	Best Update Period	4	5	4	7	7	7	7	7

		Smoothness Score	4,896	3,868	3,192	2,664	2,499	2,449	2,449	2,449
	100	Best Update Period	4	5	4	7	5	5	4	2
		Smoothness Score	4,818	3,699	2,777	2,214	1,688	1,382	1,270	957
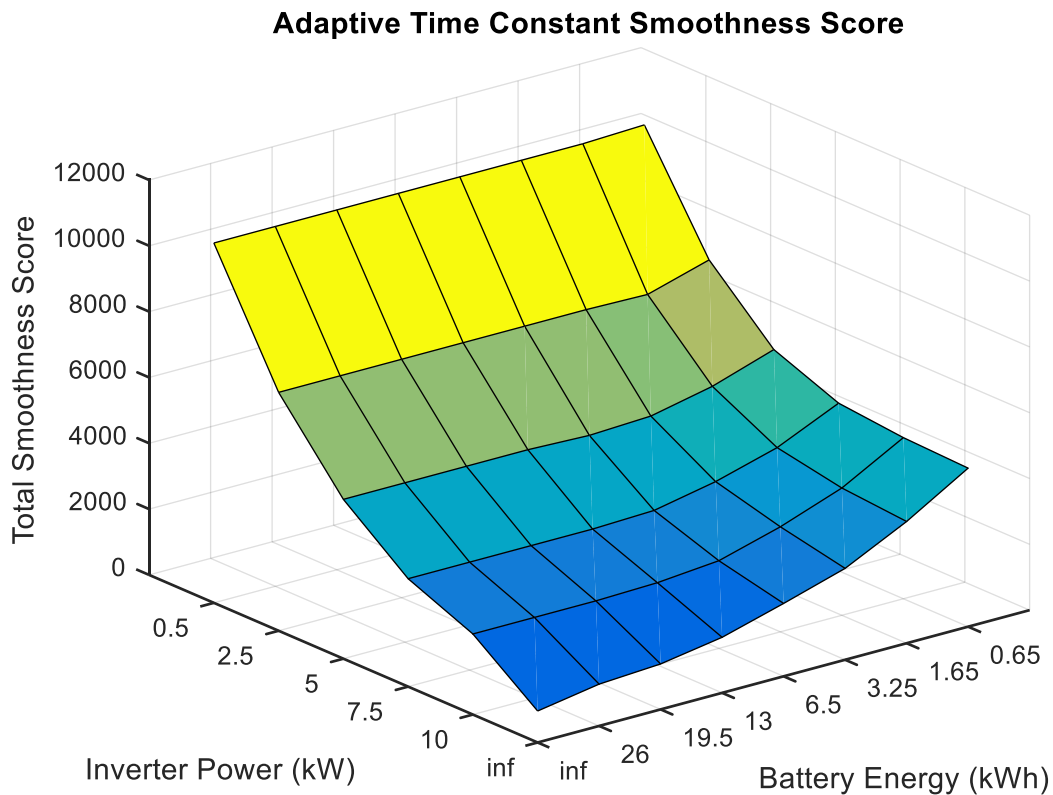
Figure 18: Smoothness Score versus BESS limitations over 26 Days for Adaptive Time Constant Selection Method

It can be observed that 7 days is most frequently the best update period. This is in part because systems where the best update period may be greater than 7 days are grouped in this category as this update period was the best of those analyzed. It is also notable that configurations with limited BESS resources tend to perform better with shorter update periods. This is because these systems are more dependent on the sun and cloud cover patterns, and therefore the best time constant may change more frequently than systems with more available inverter power and battery energy.

The trends exhibited when using adaptive time constant selection are similar to the ideal and static time constant cases. Smoothness score decreases with increased inverter power and battery energy, though there is a limit to how much battery energy would benefit the system. This limit depends on the inverter power, as with the previously discussed cases.

To compare the results of the adaptive approach with the ideal case and the static approach, the percent error between the ideal case and adaptive approach was calculated. This represents how much higher the smoothness score for the adaptive method is. The percent error for the best update period at each BESS configuration is calculated in Table 14.

Table 14: Adaptive Time Constant Selection Method Percent Error

Percent Error (%)		Battery Energy (kWh)							
		0.65	1.625	3.25	6.5	13	19.5	26	325
Inverter Power (kW)	0.5	1.35	1.39	1.39	1.39	1.39	1.39	1.39	1.39
	2.5	4.87	2.80	4.79	5.41	5.51	5.51	5.51	5.51
	5	4.28	6.14	4.78	6.57	9.39	9.39	9.39	9.39
	7.5	4.71	6.34	7.60	5.84	7.64	9.03	9.26	9.26
	10	4.71	6.40	9.34	8.56	10.61	11.77	13.28	13.28
	100	4.57	6.87	8.05	16.57	18.78	17.90	18.86	5.04

The percent error for adaptive time constant selection with this distribution of parameters ranges from 1.35% to 18.86%. Table 15 shows the mean and variance of this percent error using the best update period, as well as using a constant update period across all parameters.

Table 15: Mean and Variance of Percent Error across BESS Constraint Parameters, Adaptive Time Constant Selection Method

Update Period (Days)	Mean Percent Error	Variance
1	40.44%	1624
2	13.84%	99.81
3	11.30%	103.7
4	13.23%	191.4
5	10.89%	77.01
6	13.60%	130.1
7	8.87%	39.09

Raw PV	408.29%	-
Best	**7.19%**	**20.84**

Table 15 shows that the mean percent error trends downward as the update period increases, with the 7-day update period yielding the lowest mean percent error and variance among constant update periods. While adapting the update period based upon system parameters further reduces this percent error, this is indication that assigning an update period of 7 days (or greater) on average will provide better smoothing results than shorter periods.

7.3.3 Comparison of Time Constant Selection Methods

Both the static and adaptive methods of time constant selection produce results much smoother than the raw PV measurements, though neither match the performance of the ideal case where τ_{best} for each day is known ahead of time. This is summarized in Table 16, which compares system performance using the mean percent error across all BESS parameter combinations analyzed.

Table 16: Comparison of Time Constant Selection Method Percent Error

Time Constant Selection Method	Mean Percent Error
Raw PV	408.29%
Ideal Case	0.00%
Static Method	5.71%
Adaptive Method	7.19%

According to these results, while both time constant selection methods greatly improve performance compared to the raw unfiltered PV generation measurements, the static selection method outperforms the adaptive selection method by 1.48% on average.

It should be noted that there are considerations regarding the dataset to take into account when comparing the two methods. This study used 26 sequential days of PV generation data. For the static method, part of this data was used for historical data over which to calculate the time constant, and therefore the set of data which yielded the best result could have benefited the total smoothness score of the system. However, this data was included so that the final scores would consider all 26 days and therefore be comparable to the adaptive method.

By contrast, the adaptive method assigned a default initial time constant during the first period before time constant calculation, which may or may not have been the best time constant for that duration.

For comparison, if the best time constant for the first update period is assigned (making the assumption that this value is somehow known ahead of time), the mean percent error of the smoothness score drops from 7.19% to 6.27%. Therefore, making this unrealistic assumption in an attempt to counteract the benefit the static method receives in its calculation still does not allow the adaptive method to surpass the static.

The static method performs better than the adaptive because of the weakness of the following assumption: the best time constant for a given period of time will also perform well for the next period of time due to slowly changing weather patterns. In reality, solar and cloud cover patterns are highly variable, and are subject to change. A large period of time is required in order to make an assessment regarding the best time constant, and for the adaptive method, this means that there will be a longer period of time before the next update where new patterns can be considered.

To learn if the delay between time constant updates is the cause for poor performance of the adaptive method, one variation was analyzed with a rolling historical window to compare with the 7-day update method. In this method, time constant selection occurs every day, but considers the past 7 days of data. Using this method, the mean percent error was 8.80%. This is an improvement over using a constant 7-day update, which yielded 8.87%, but it does not improve over choosing the best update period (7.19%). This indicates that the delay between time constant updates is not the primary reason for poor adaptive performance. This is a topic that may be explored further nonetheless

However, even given the superior performance of the static method, there are other considerations as well. The static time constant was calculated for the 26-day period, but longer-term changes in weather patterns could have the potential to drift away from this value. If a location has strong seasonal patterns, the best filter may change several time throughout the year. In contrast, a location with weaker seasonal changes may do well with a static time constant.

7.4   Real-Time Operation

The PV Smoothing System is constructed using the agent architecture shown in Figure 1 across two computers running VOLTTRON™. The host computer runs device communications functions as well as the Energy Cost Optimization System, and a peripheral computer runs the PV Smoothing System. The two systems communicate using the VIP protocol to extend the message bus. The Energy Cost Optimization System operates at a clock cycle of 5 minutes, while the PV Smoothing System operates at 1 second.

The BESS contribution towards the PV Smoothing System was limited to 5 kW/6.5 kWh, or 5 percent of the total inverter power and 2 percent of the total battery energy capacity. These levels were chosen to demonstrate the impacts of limited BESS resources.

The adaptive approach to time constant selection was chosen in order to demonstrate the adaptive filter tuning agent. Referencing Table 13, a 7-day update period was chosen. The initial time constant chosen was $\tau = 400$, which was updated after 7 days of operation.

Real-time PV smoothing using VOLTTRON™ is shown for a day in Figure 19. The data in this figure was taken before the 7-day window was complete, so the time constant remains at $\tau = 400$.
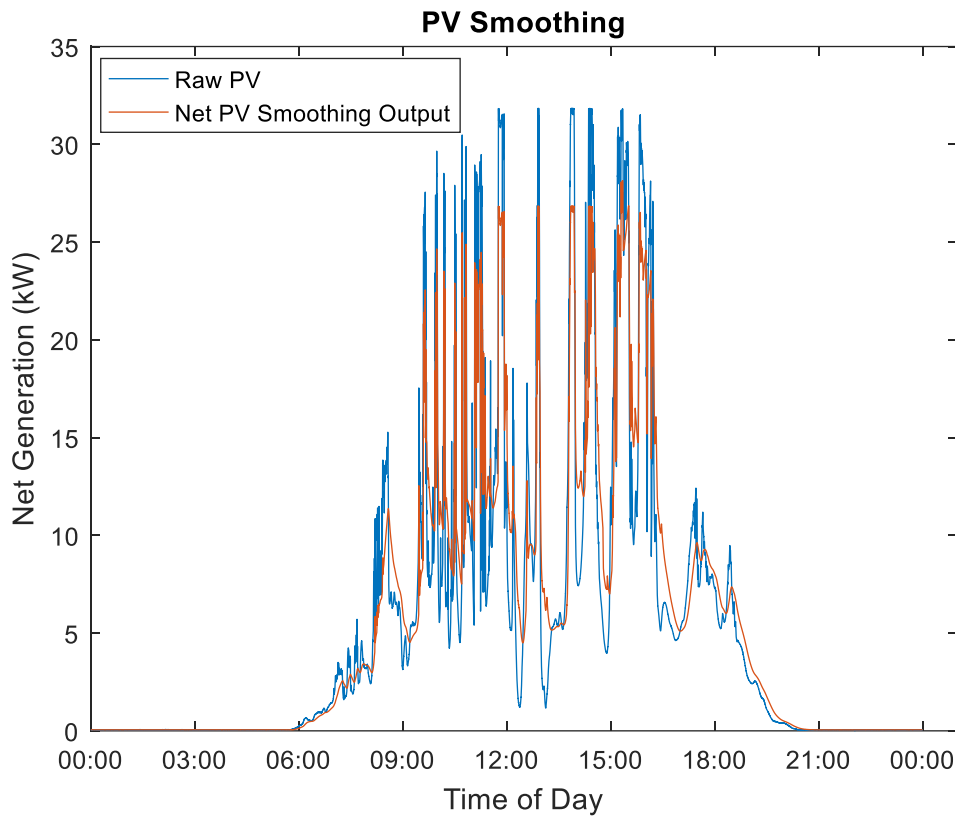
Figure 19: Real-Time Smoothing Using VOLTTRON™, May 12th, 2017. Initial Time Constant $\tau = 400$

It can be seen that with this time constant, PV smoothing does occur, as fast variations in the PV generation are flattened. However, variations in the middle of the day reach magnitudes of 20 kW, and cannot be adequately smoothed with the constraints placed on the BESS. The resulting smoothness scores of the raw data and smoothed result are shown in Table 17.

Table 17: Real-Time Smoothing Results Using VOLTTRON, May 12th, 2017

System Characteristic	Smoothness Score
Raw PV Generation	1,994.8
Net Smoothed Generation	1,083.3

It can be seen that system variations were nearly cut in half with the implementation of PV smoothing, even with the limitations on the BESS.

Shows some of the most extreme variations of this day in closer detail to demonstrate these limitations.
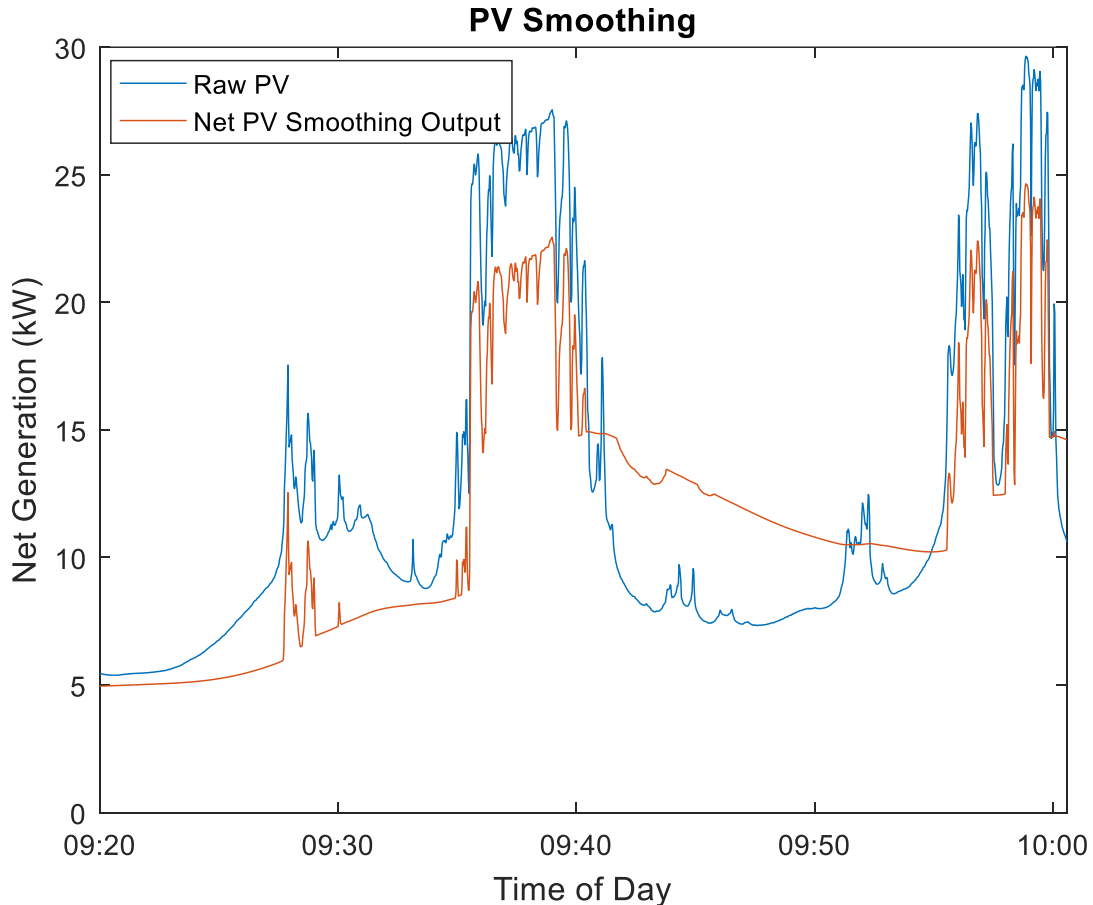

Figure 20: Real-Time Smoothing Using VOLTTRON™, May 12th, 2017, Focus on Large Variations

It can be seen from this figure that the BESS limitations on inverter power are restricting the smoothing operation. Where smoothing for the lower-magnitude variations is effective, the large increase in output power around 9:35 a.m. creates a power difference between the PV generation and desired smoothing curve that cannot be rectified by the BESS output. The difference between the two curves at any given point is limited to 5 kW because this is the limitation placed on the inverter output, which can be seen in Figure 20.

The BESS is shared between two real-time systems. Figure 21 and Figure 22 depict the state of the BESS at all points throughout May 12th, 2017.
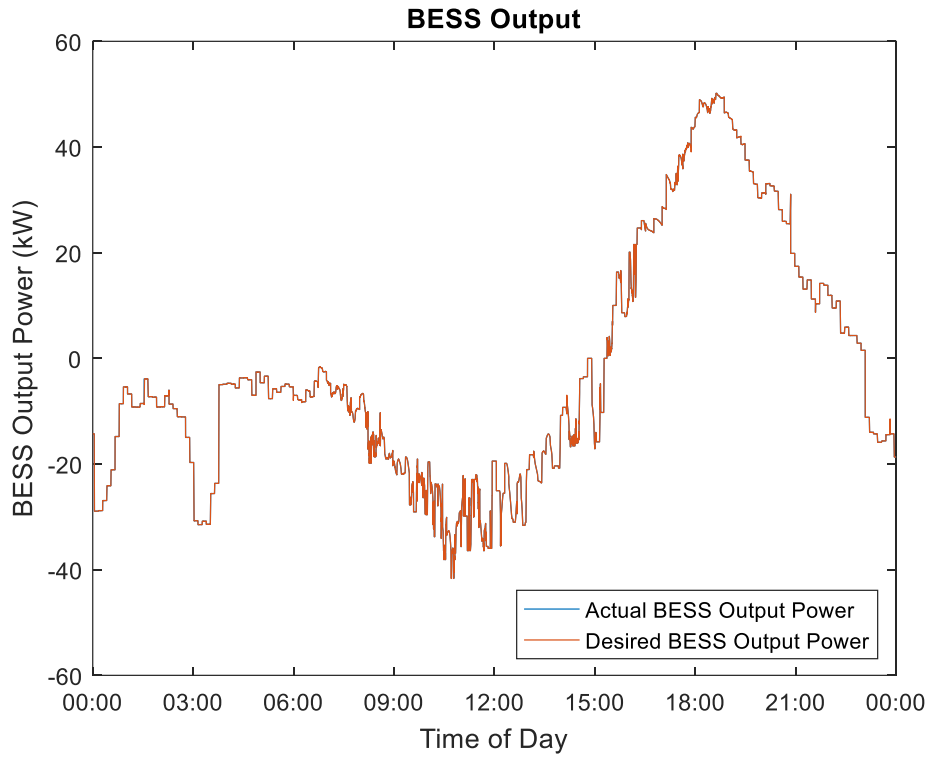
Figure 21: Desired versus Actual BESS Output Power, May 12th, 2017
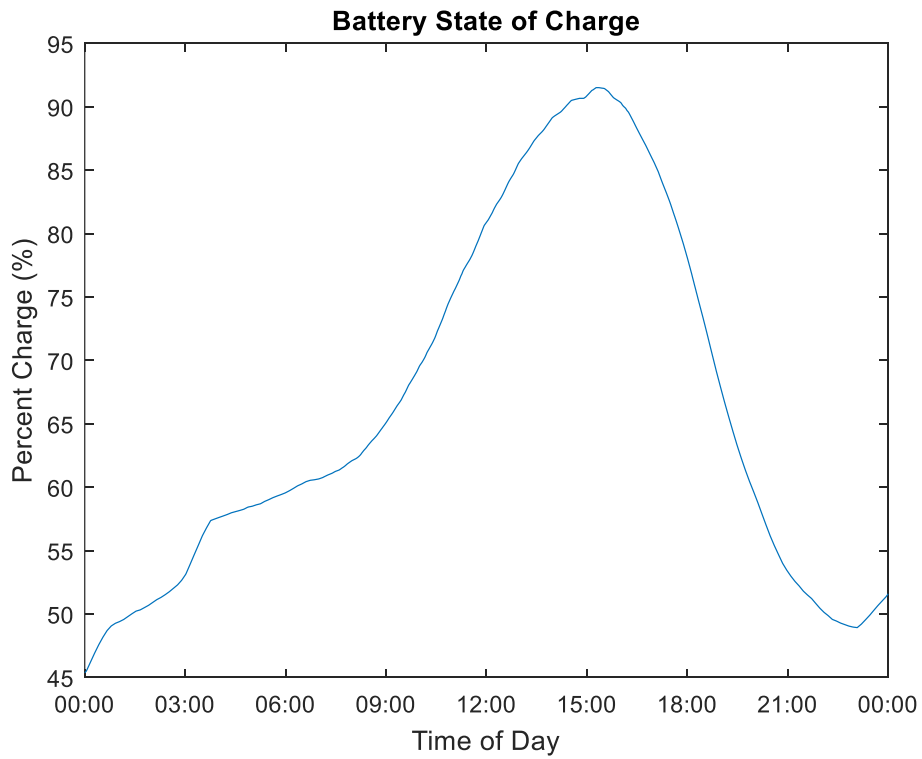
Figure 22: State of Charge of BESS, May 12th, 2017

Figure 21 shows that the desired BESS output matches the actual output at every time step. It depicts the BESS supporting both systems simultaneously: the Energy Cost Optimization System and the PV Smoothing System. It can be seen that the BESS output is segmented as a step function: this is because the Energy Cost Optimization System runs at a 5-minute resolution, so the output is held constant for 300 clock cycles of the PV Smoothing System. However, as the variations in PV generation increase in magnitude during the peak solar hours, the PV smoothing signal is noticeable as high frequency variations in BESS output power.

As can be seen in Figure 22, the SOC never reaches its maximum or minimum capacity. This is the reason for the zero discrepancy between desired and actual power, as the BESS should only deviate from the requested power output when it approaches its own capacity limitations. Should the SOC approach 100%, there may develop an increased mismatch between the desired and actual BESS output.

After the update period elapses, the message visible in the logged output of the VOLTTRON™ terminal is shown in Figure 23.


```
INFO: Result Evaluation Complete for T= 100 . Linear grade is 5146.001456
INFO: Result Evaluation Complete for T= 200 . Linear grade is 5090.446292
INFO: Result Evaluation Complete for T= 400 . Linear grade is 5108.941888
INFO: Result Evaluation Complete for T= 800 . Linear grade is 5426.316604
INFO: Result Evaluation Complete for T= 1600 . Linear grade is 6789.415032
INFO: Result Evaluation Complete for T= 2400 . Linear grade is 8077.790304
INFO: T_message is [{'Second': 604884, 'TimeConstant': 200}, {'Second': {'
```

Figure 23: VOLTTRON™ Log Output during Adaptive Time Constant Update

The information provided by this output is summarized in Table 18.

Table 18: VOLTTRON™ Log Output Summary

Time Constant	7-Day Smoothness Score
100	5146
200	5090
400	5109
800	5426
1600	6789
2400	8078
τ_{best}	**200**

From Table 18, it can be seen that the best time constant is $\tau_{best} = 200$. This is because filters with a longer time constant than this attempt to smooth too aggressively for the constraints placed on the

BESS. As can be seen in Figure 20, a filter with $\tau = 400$ frequently reaches its inverter limit. Therefore, for the duration of the next update period the filter will use $\tau = 200$. Operation after this point is shown in Figure 24.
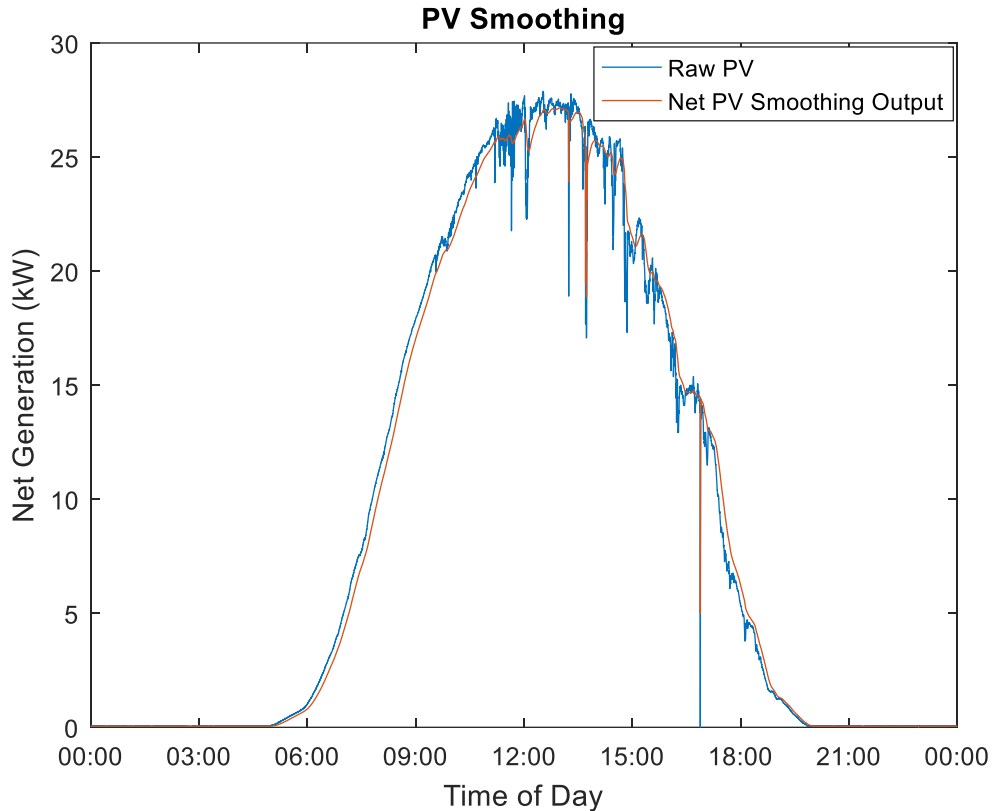
Figure 24: Real-Time Smoothing using VOLTTRON™, after Time Constant Update to $\tau = 200$

Variations on this day are less severe than in Figure 20, and with the updated time constant the system is better able to accommodate variations in PV output. The system will run indefinitely from this point, updating the time constant every 7 days in order to stay current with seasonal and weather patterns. Thus, the real-time implementation of the PV Smoothing System in VOLTTRON™ has been demonstrated. The figures presented here also depict VOLTTRON™, simultaneously performing two functions: PV smoothing and the larger Energy Cost Optimization System.

VIII Conclusion

This project has demonstrated the capabilities of VOLTTRON™ when used as a control system for distributed energy resources operating two simultaneous functions. Specifically, the system manages an Energy Cost Optimization System using scheduled BESS dispatch, as well as the PV Smoothing System described in this study.

The system was thoroughly analyzed using 26 days of PV generation at 1-second resolution. The effect of changing the time constant of the filter during constrained and unconstrained operation was analyzed. Next, the impact of BESS constraints on smoothness and best time constant were studied in an ideal setting where the best time constant is known prior to a day's operation. It was determined that having a large inverter output power was more important for PV smoothing than a large battery energy capacity.

Two methods of selecting the time constant in real time, static and adaptive, are studied for their impact on system performance. The static method uses one set of historical data to assign a permanent time constant to the system, while the adaptive method recalculates this time constant after a certain window of time. It was found that both systems provide a high level of PV smoothing performance. However, the static method can decrease variations within 5.7% of the ideal case, while the adaptive method decreases variations down to within 7.2%. The location and seasonal weather patterns should also be considered when choosing between the two methods of time constant selection.

The system was then run in real time using VOLTTRON™. At BESS limitations of 5 kW/6.5 kWh, the best adaptive update period was determined to be 7 days. The system behaved as expected given the BESS parameters and time constant selection methods, providing smoothing on the PV generation and updating the time constant periodically using the adaptive time constant selection method.

This project paves the way for future work in the area of real-time PV smoothing, including:

- o Studying the output characteristic of BESS hardware in place of a mathematical physics-based model, including response time analysis
- o Investigating realistic costs of power ramping on the grid to determine an appropriate smoothness penalty function
- o Expanding the data set to investigate monthly and seasonal changes in system behavior
- o An adaptive time constant selection method featuring daily time constant updates while using a longer period of time as the historical data for such updates
- o Investigating tools for predicting variations in PV generation variance
- o Investigating larger PV generation, including arrays over a larger geographic area
- o Investigating shorter time frames for PV variability behavior and PV smoothing

X References

[1] B. Obama, "The irreversible momentum of clean energy," *Science*, 2017.

[2] F.R. Pazheri, M.F. Othman and N.H. Malik, "A review on global renewable electricity scenario," *ScienceDirect*, 2014.

[3] P. Denholm and M. Hand, "Grid flexibility and storage required to achieve very high penetration of variable renewable electricity," *ScienceDirect Energy Policy*, 2011.

[4] L. Hirth, F. Ueckerdt and O. Edenhofer, "Integration costs revisited – An economic framework for wind and solar variability," *ScienceDirect Renewable Energy*, 2014.

[5] APS Panel on Public Affairs, "Integrating Renewable Electricity on the Grid," American Physical Society, 2011.

[6] A. Mills, M. Ahlstrom, M. Brower, A. Ellis, R. George, T. Hoff, B. Kroposki, C. Lenox, N. Miller, J. Stein and Y. Wan, "Understanding Variability and Uncertainty of Photovoltaics for Integration with the Electric Power System," Ernest Orlando Lawrence Berkeley National Laboratory, 2009.

[7] "VOLTTRON", Pacific Northwest National Laboratory [Online]. Available: http://bgintegration.pnnl.gov/volttron.asp.

[8] M. Starke, J. Nutaro, T. Kuruganti and D. Fugate, "Integration of Photovoltaics into Building Energy Usage through Advanced Control of Rooftop Units," *International High Performance Buildings Conference,* 2014.

[9] J. Apt, "The Spectrum of Power from Wind Turbines," Carnegie Mellon Electricity Industry Center Working Paper, 2007.

[10] Y. Moumouni, Y. Baghzouz and R. F. Behm, "Power 'Smoothing' of a Commercial-Size Photovoltaic System by an Energy Storage System," IEEE International Conference on Harmonics and Quality of Power, 2014.

[11] E. Balamurugan and S. Venkatasubramanian, "Analysis of Double Moving Average Power Smoothing Methods for Photovoltaic Systems," *International Research Journal of Engineering and Technology*, 2016

[12] X. Li, D. Hui and X. Lai, "Battery Energy Storage Station (BESS)-Based Smoothing Control of Photovoltaic (PV) and Wind Power Generation Fluctuations," *IEEE Transactions on Sustainable Energy, Vol. 4, No. 2*, 2013.

[13] L. Xu, X. Ruan, C. Mao, B. Zhang and Y. Luo, "An Improved Optimal Sizing Method for Wind-Solar-Battery Hybrid Power System," *IEEE Transactions on Sustainable Energy, Vol. 4, No. 3*, 2013.

[14] S. Tewari and N. Mohan, "Value of NAS Energy Storage Toward Integrating Wind: Results From the Wind to Battery Project," *IEEE Transactions on Power Systems, Vol. 28, No. 1*, 2013.

[15] T. D. Hund, S. Gonzalez and K. Barrett, "Grid-Tied PV System Energy Smoothing," IEEE Photovoltaic Specialists Conference, 2010.

[16] C. A. Hill, M. C. Such, D. Chen, J. Gonzalez and W. M. Grady, "Battery Energy Storage for Enabling Integration of Distributed Solar Power Generation," *IEEE Transactions on Smart Grid, Vol. 3, No. 2*, 2012.

[17] E. Hittinger, J. F. Whitacre and J. Apt, "Compensating for wind variability using co-located natural gas generation and energy storage," *Energy Systems*, 2010.

[18] B. Akyol, J. Haack, S. Ciraci, B. Carpenter, M. Vlachopoulou and C. Tews, "VOLTTRON: An Agent Execution Platform for the Electric Power System," *ResearchGate,* 2012.

[19] J. Haack, B. Akyol, B. Carpenter, C. Tews and L. Foglesong, "Volttron: An Agent Platform for the Smart Grid (Demo)," *International Foundation for Autonomous Agents and Multiagent Systems*, 2013.

[20] V. Chinde, A. Kohl, A. Jiang, A. Kelkar and S. Sarkar, "A VOLTTRON based implementation of Supervisory Control using Generalized Gossip for Building Energy Systems," *International High Performance Buildings Conference,* 2016.

[21] J. Sanyal, D. Fugate, K. Woodworth, J. Nutaro and T. Kuruganti. "Embedded Volttron Specification – Benchmarking Small Footprint Compute Devices for Volttron," Oak Ridge National Laboratory, 2015.

[22] R. Singh, A. Hahn and C. Liu, "Managing Distributed Energy Resources Using VOLTTRON: A case study of the WSU CETC Project," Washington State University, 2016.

[23] M. Ortega-Vazque, "Optimal scheduling of electric vehicle charging and vehicle-to-grid services at household level including battery degradation and price uncertainty," *IET Generation, Transmission & Distribution, Vol. 8, Iss. 6*, 2014.

[24] T. Sasaki, Y. Ukyo and P. Novak, "Memory effect of a lithium-ion battery," *Nature Materials*, 2013.

[25] O. Tremblay and L. A. Dessaint, "Experimental Validation of a Battery Dynamic Model for EV Applications," *World Electric Vehicle Journal, Vol. 3*, 2009.

[26] N. Kawasaki, T. Oozeki, K. Otani and K. Kurokawa, "An evaluation method of the fluctuation characteristics of photovoltaic systems by using frequency analysis," *ScienceDirect Solar Energy Materials & Solar Cells*, 2006.

XI   Appendix

The appendix for this thesis is available as in the form of the file:

"Kevin_Morrissey_PV_Smoothing_Appendix.zip"

The contents of the appendix are as follows:

- raw_PV_generation_measurements.csv
  - 26 days of 1-second increment PV generation measurements from a 35-kW PV array on UW campus. This dataset was used for simulation analysis of the PV Smoothing System.
- PVsmoothing
  - Folder containing the VOLTTRION™ code associated with the PV Smoothing System
  - Contains two VOLTTRON™ agents:
    - real_time_filter
      - VOLTTRON™ agent that performs real-time filtering on PV generation measurements and dispatches a BESS instruction each to execute this.
      - config: A configurable file featuring all parameter inputs into the PV Smoothing System.
    - adaptive_filter_tuning
      - VOLTTRON™ agent that recalculates the best time constant based on a historical period of data and submits the updated time constant value to the real_time_filter agent in real time.